HHS Public Access

Author manuscript

Dev Biol. Author manuscript; available in PMC 2018 May 16.

Published in final edited form as:

Dev Biol. 2017 January 01; 421(1): 52–66. doi:10.1016/j.ydbio.2016.10.019.

The *tbx2a/b* transcription factors direct pronephros segmentation and corpuscle of Stannius formation in zebrafish

Bridgette E. Drummond[1], **Yue Li**[1], **Amanda N. Marra**, **Christina N. Cheng**, **Rebecca A. Wingert**[*]

Department of Biological Sciences, Center for Stem Cells and Regenerative Medicine, Center for Zebrafish Research, University of Notre Dame, Notre Dame, IN 46556, USA

Abstract

The simplified and genetically conserved zebrafish pronephros is an excellent model to examine the cryptic processes of cell fate decisions during the development of nephron segments as well as the origins of associated endocrine cells that comprise the corpuscles of Stannius (CS). Using whole mount *in situ* hybridization, we found that transcripts of the zebrafish genes *t-box 2a* (*tbx2a*) and *t-box 2b* (*tbx2b*), which belong to the T-box family of transcription factors, were expressed in the caudal intermediate mesoderm progenitors that give rise to the distal pronephros and CS. Deficiency of *tbx2a*, *tbx2b* or both *tbx2a/b* reduced the size of the distal late (DL) segment, which was accompanied by a proximal convoluted segment (PCT) expansion. Further, *tbx2a/b* deficiency led to significantly larger CS clusters. These phenotypes were also observed in embryos with the *from beyond (fby)*^{c144} mutation, which encodes a premature stop codon in the *tbx2b* T-box sequence. Conversely, overexpression of *tbx2a* and *tbx2b* in wild-type embryos expanded the DL segment where cells were comingled with the adjacent DE, and also decreased CS cell number, but notably did not alter PCT development—providing independent evidence that *tbx2a* and *tbx2b* are each necessary and sufficient to promote DL fate and suppress CS genesis. Epistasis studies indicated that *tbx2a* acts upstream of *tbx2b* to regulate the DL and CS fates, and likely has other targets as well. Retinoic acid (RA) addition and inhibition studies revealed that *tbx2a* and *tbx2b* are negatively regulated by RA signaling. Interestingly, the CS cell expansion that typifies *tbx2a/b* deficiency also occurred when blocking Notch signaling with the chemical DAPT (N-[N-(3,5-difluorophenacetyl)-L-alanyl]-S-phenylglycine t-butyl ester). Ectopic activation of Notch in *Tg*(*hsp70::Gal4; UAS::NICD*)(NICD) embryos led to a reduced CS post heat-shock induction. To further examine the link between the *tbx2a/b* genes and Notch during CS formation, DAPT treatment was used to block Notch activity in *tbx2a/b* deficient embryos, and *tbx2a/b* knockdown was performed in NICD transgenic embryos. Both manipulations caused similar CS expansions, indicating that Notch functions upstream of the *tbx2a/b* genes to suppress CS ontogeny. Taken together, these data reveal for the first time that *tbx2a/b* mitigate pronephros segmentation downstream of RA, and that interplay between Notch signaling and *tbx2a/b* regulate CS formation, thus providing several novel insights into the genetic regulatory networks that influence these lineages.

[*]Correspondence to: Department of Biological Sciences, University of Notre Dame, 100 Galvin Life Sciences, Notre Dame, IN 46556, USA. rwingert@nd.edu (R.A. Wingert).

[1]Equal authors.

Keywords

Kidney; Pronephros; Nephrogenesis; Epithelial cell fate; Nephron segments; Corpuscle of Stannius; *tbx2a* ; *tbx2b* ; *sim1a* ; Retinoic acid; Notch signaling

1. Introduction

Kidneys are excretory organs with an intricate architecture and a rich diversity of cell types. Typically, renal cells are arranged into functional units known as nephrons, while other cells constitute interstitial supporting populations. Vertebrate kidney development progresses through a series of two or three stages, depending on the species, in which a pronephros, mesonephros, and a metanephros are formed (Saxen, 1987). Each kidney organ is composed of nephrons, though their numbers increase and their arrangements are progressively more complex with each successive stage (Dressler, 2006). For example, in mammals the pronephros and mesonephros contain up to several dozen nephrons that are situated in parallel arrays, while the ensuing adult metanephric kidney has thousands or even millions of nephrons that are organized in elaborate arborized configurations (Takasato and Little, 2015).

At present, one major aspect of vertebrate kidney development that remains largely enigmatic is how nephron tubular epithelial cells acquire segment-specific fates during nephrogenesis. The meager understanding of nephron segmentation is due in part to the complexity of mammalian kidney anatomy and limited models to study nephrogenesis *in vitro* (Costantini and Kopan, 2010). However, nephron structure is broadly conserved among vertebrates (Romagnani et al., 2013). Furthermore, in recent years there has been an increasing appreciation of the usefulness of the zebrafish pronephros as a simplified, genetically tractable experimental system for nephrogenesis studies in the context of organ development and regeneration (Drummond and Wingert, 2016).

The embryonic zebrafish kidney is a functional pronephros composed of two nephrons that form rapidly, becoming segmented into phenotypically distinct regions by 24 hours post fertilization (hpf) (Gerlach and Wingert, 2013). Each segment plays discrete and essential roles in renal physiology including, but not limited to, the absorption and secretion of particular metabolites and electrolytes, which is mediated by the expression of solute transporters (Ebarasi et al., 2011). It has been shown that the solute transporter genes that are expressed in each pronephric segment correspond with genes that are expressed in similar segments in nephrons of the mature mammalian kidney, thereby establishing the relevance for segmentation research using zebrafish (Wingert et al., 2007; Wingert and Davidson, 2008). These segments include the podocytes (P), neck (N), proximal convoluted and straight tubule (PCT, PST), distal early and late (DE, DL) tubule, and a pronephric duct (PD) (Wingert et al., 2007; Wingert and Davidson, 2008). In zebrafish, nephron segment patterning is known to be reliant on retinoic acid (RA), produced largely from the paraxial mesoderm, which divides the renal progenitor field (derived from the intermediate mesoderm) into rostral and caudal domains that are further induced to form the series of tubule segments (Wingert et al., 2007; Wingert and Davidson, 2011). The ongoing

application of the zebrafish pronephros model has begun to further elucidate the cast of key transcription factors and signaling pathways that are expressed by developing nephron segments, and defined a growing number of their functional roles, such as Notch signaling in governing tubule epithelial fate choices (Ma and Jiang, 2007; Liu et al., 2007; O'Brien et al., 2011; Naylor et al., 2013; Kroeger and Wingert, 2014; Li et al., 2014; Gerlach and Wingert, 2014; McKee et al., 2014; Marra and Wingert, 2014, 2016; Miceli et al., 2014; Cheng and Wingert, 2015).

In addition to the pronephros, the intermediate mesoderm field gives rise to groups of endocrine cells called the corpuscles of Stannius (CS) that are initially located in the vicinity of the DE and DL segment precursors and then later coalesce into a pair of clustered organs that are situated dorsal to the pronephros (Elizondo et al., 2005; Wingert et al., 2007). The CS are endocrine glands found in bony fish (Garrett, 1942; Krishnamurthy, 1976). The CS are responsible for the synthesis and secretion of stanniocalcin 1 (STC1), a glycoprotein hormone that regulates calcium and phosphate homeostasis in fishes through its actions on the gills and kidneys (Elizondo et al., 2005; Krishnamurthy, 1976; Kaneko et al., 1992). As such, the CS are thought to be important regulators of calcium uptake from the aquatic environment (Elizondo et al., 2005). Although the CS and the proteins they secrete were previously considered to be an endocrine system that is unique to fishes, intriguing evidence has implicated the existence of STC-like proteins in humans and other higher vertebrates (Wagner et al., 1995; Chang et al., 1995). To date, however, not much is known about the genetic factors that induce the CS lineage or regulate its differentiation. CS fate is reliant on RA signaling within the zebrafish embryo, where elevated RA levels block CS formation and RA biosynthesis abrogation expands the CS (Wingert et al., 2007). More recently, the *single-minded family bHLH transcription factor 1a* (*sim1a)* was discovered to be both necessary and sufficient for CS formation, and shown to act downstream of RA in promoting *stc1*-expressing cell fate (Cheng and Wingert, 2015).

In searching for other candidate nephron segmentation modulators, we noticed that expression of the *t-box 2b* (*tbx2b*) transcription factor was annotated within the distal pronephros at 24 hpf during zebrafish embryogenesis, similar to its paralog *t-box 2a* (*tbx2a*) (Dheen et al., 1999; Thisse and Thisse, 2004; Slanchev et al., 2011; Thu et al., 2013), in an area that is now known to correspond to the site of the distal tubule, duct, and CS (Wingert et al., 2007). Interestingly, *in situ* hybridization showed *Tbx2* expression in the mesonephros and also in the E12.5 metanephric tubules of the developing murine kidney (Chapman et al., 1996). More recently, *Tbx2* expression was also reported in the ureteric bud tips (GUDMAP: 10896), which give rise to the collecting duct system (Little and McMahon, 2012). Previous research in *Xenopus* has shown that *Tbx2* loss of function results in an enlarged pronephros, whereas ectopic activation of *Tbx2* inhibits nephric mesoderm differentiation in embryos (Cho et al., 2011). Further, *Tbx2* repressed expression of the Notch factor *Hey1* to control pronephric morphogenesis, suggesting a link between *Tbx2* and Notch during nephrogenesis in *Xenopus* (Cho et al., 2011). Until the present study, however, no one had examined the roles of *tbx2a/b* in nephron segment formation.

Here, we identified *tbx2a* and *tbx2b* as essential regulators of pronephros and CS development. Gene knockdown studies and analysis of the *tbx2b* mutant *from beyond*

(fby^{c144}) showed that loss of one or both *tbx2a* and *tbx2b* led to a short DL segment and significantly larger CS clusters. Further, overexpression of *tbx2a* or *tbx2b* was sufficient to expand the DL and significantly reduce CS cell number. Epistasis experiments revealed that *tbx2a* acts upstream of *tbx2b*, and suggested that *tbx2a* mitigates the DL and CS lineages by regulating an additional target(s) as well. In testing the relationship of *tbx2a/b* genes with previously known nephron patterning pathways, we determined that RA signaling negatively regulates their spatiotemporal expression. Finally, we found that Notch signaling is essential to restrict CS fate, and that the *tbx2a/b* transcription factors act downstream of Notch to repress CS formation. In sum, this research has identified new roles for *tbx2a/b* in nephron segmentation, and revealed for the first time that Notch signaling and *tbx2a/b* modulate CS genesis.

2. Materials and methods

2.1. Zebrafish husbandry and ethics statement

Zebrafish were housed in the Center for Zebrafish Research at the University of Notre Dame Freimann Life Science Center. The Institutional Animal Care and Use Committee (IACUC) approved studies all under protocols 16–025 and 16-07-3245. Wild-type Tübingen, *fby^{c144}*, and *hsp70::Gal4; UAS::NICD* adults and embryos were maintained and staged as previously described (Westerfield, 1993; Kimmel et al., 1995). Embryos were raised in E3 medium (5 mM NaCl, 0.17 mM KCl, 0.33 mM $CaCl_2$, 0.33 mM $MgSO_4$) at 28 °C (Westerfield, 1993).

2.2. Whole mount and fluorescence in situ hybridization

Whole mount *in situ* hybridization was performed as described (Cheng et al., 2014). Antisense riboprobes were generated for *smyhc1, slc12a1, slc12a3, slc20a1a, trpm7, stc1*, and *sim1a*, as previously reported (Wingert et al., 2007; Cheng and Wingert, 2015). The DNA template for the *tbx2a* riboprobe was generated from IMAGE clone 6964146 using the PCR primers (5′-ATGGCTTATCACCCTTTTCACGCGCACAGGCCGGCCG-3′ and 5′-ATTAACCCTCACTAAAGGGCTCTCCCAGTAGTTGTTCGCAAGATGAGTCGTCCGA-3′). The DNA template for *tbx2b* was generated from IMAGE clone 5914621 with PCR primers (5′-ATGAGAGATCCAGTTTTTAC-3′, 5′-AATTAACCCTCACTAAAGGTCATTTGGGTGA-3′). PCR products were purified using the Qiagen PCR purification kit and riboprobes generated using t3 RNA polymerase. Detection was performed using antidigoxigenin and anti-fluorescein antibody (Roche) and NBT/BCIP/INT staining reagents. Fluorescent whole mount *in situ* hybridization was performed as described (Brend and Holley, 2009).

2.3. Morpholinos

All morpholino oligonucleotides were obtained from Gene Tools, LLC. *tbx2a* splice morpholino was designed to target the splice acceptor site of exon 1 (5′-GGAAACATTCTCCTATGGACGAAAG-3′) (Thu et al., 2013). *tbx2b* splice morpholino was designed to target the splice donor site of exon 3 (5′-AAAAATATGGGTACATACCTTGTCGT-3′) (Gross and Dowling, 2005). The following start site targeting morpholinos were used: *tbx2a* ATG morpholino (5′-ATCGGTGCATCCAAAAAGCCAGAT-3′) (Ribeiro et al., 2007); *tbx2b* ATG morpholino

(5′-CCTGTAAAAACTGGATCTCTCATCGG-3′) (Gross and Dowling, 2005); *tbx2ab* ATG morpholino (5′-AAAACTGGATCTCTCATCGGTGCAT-3′) (Sedletcaia and Evans, 2011). Embryos at the 1-cell stage were injected with approximately 2 nl of morpholino from a 0.25 mM dilution. Injected embryos were incubated at 28 °C until fixation in 4% paraformaldehyde/PBST at the 28 ss. Embryos undergoing gene expression analysis were stored in methanol at −20 °C.

2.4. RT-PCR

RNA was extracted from 24 hpf *tbx2a* and *tbx2b* splice morphants using Trizol (Invitrogen). For *tbx2a* morphant and control cDNA, primers were used to amplify exons 1–3 of *tbx2a* (5′-GGCTGA AGCTGGTTTACACGCGGCGCTTGGACATCACCACCAGGCGGCTCAT-3′ and 5′-GTCGTTGGCTCTAACGATATGAAACCTGGGTTGGTATTTG TGCATTGAATTTA-3′). Regions within exon 2–4 of *tbx2b* were amplified in cDNA from *tbx2b* splicing morphants and controls using PCR primers (5′-TAAACTGAAGTTAACCAACAATATTTCGGACAAACATGGATTT-3′ and 5′-CTTTTTTCTCTCCTTCCATTCCCCGTGTCTCTGAAGCCTTTGGC-3′). Gel electrophoresis was used to visualize RT-PCR products. All product bands were extracted and purified (QIAquick MinElute) and sequenced.

2.5. Overexpression studies

The open reading frames of zebrafish *tbx2a* and *tbx2b* were subcloned into the pCS2 vector. To prepare for *in vitro* transcription reactions, the *tbx2a* template was linearized using NotI restriction enzyme, and the *tbx2b* template was linearized with ApaI.I. cRNA for each gene was produced using the mMessage mMachine Sp6 kit (Ambion). cRNAs were injected into 1 cell stage embryos and fixed in PFA at 24 hpf.

2.6. Chemical treatments

1 M stocks of RA and DEAB were created by dissolving compounds (Sigma-Aldrich) in 100% DMSO aliquots and stored at −80 °C (Wingert et al., 2007; Lengerke et al., 2011). For RA treatments, embryos at the 60% epiboly stage were incubated in RA/DMSO/E3 solutions until 24 hpf. Three RA treatment doses were tested; 1×10^{-6} M, 1×10^{-7} M, and 1×10^{-8} M. For DEAB treatments, 1.6×10^{-5} M DEAB/DMSO was administered to embryos at either 50% epiboly or 90% epiboly, washed off at 24 hpf, and embryos were fixed as previously described.

2.7. Genotyping and heat shock experiments

Heterozygous mutants were identified using fin clip DNA and genotyping assays as detailed in previous studies: *fby*^{c144} (Snelson et al., 2008) and *hsp70::Gal4; UAS::NICD* (Scheer and Campos-Ortega, 1999; Scheer et al., 2002). NICD heat shock experiments were conducted by incubating embryos at the 15 somite stage in 37 °C for 1 h. Embryos were then incubated at 28 °C until the 28 ss and processed as described earlier.

2.8. Cell counts and statistics

At least 15 embryos were examined for each morpholino and drug treatment experiment, which were performed in triplicate. A minimum of three genotype-confirmed mutant embryos were acquired for each condition represented. CS cell counts were taken in each of the two nephrons in the embryos examined. CS counts were averaged across three replicates for each condition and tested for significance using a non-paired *t*-test.

3. Results

3.1. Expression of tbx2a and tbx2b during zebrafish intermediate mesoderm development

Due to the teleost genome duplication event, zebrafish possess two *tbx2* genes, designated *tbx2a* and *tbx2b*, which share approximately 80% peptide identity (Sedletcaia and Evans, 2011). Previous studies have shown that *tbx2b* is strongly expressed in the distal pronephros at 24 hpf (Dheen et al., 1999; Slanchev et al., 2011). In comparison, slightly discrepant patterns of *tbx2a* have been reported in the distal pronephros, ranging from weak to strong expression in the area (Dheen et al., 1999; Thisse and Thisse, 2004; Thu et al., 2013). Despite the variations, these data suggest that *tbx2a* and *tbx2b* might be involved in nephrogenesis, which occurs during the first day of zebrafish embryo development when each bilateral stripe of intermediate mesoderm precursors are assembled into nephron segments or a closely associated CS gland (Fig. 1A; Cheng and Wingert, 2014).

To explore this, we first performed additional expression studies to clarify the spatiotemporal domains of *tbx2a* and *tbx2b* in the intermediate mesoderm. Whole mount *in situ* hybridization with RNA antisense riboprobes specific for *tbx2a* or *tbx2b* transcripts, as well as corresponding sense controls, was conducted on wild-type embryos at numerous developmental stages during the time frame when renal progenitors undergo segmental patterning (Fig. 1B, Supplementary Fig. 1). *tbx2a* and *tbx2b* transcripts were present in the caudal intermediate mesoderm as early as the 8 somite stage (ss), and were maintained in the developing pronephros through the 28 ss (Fig. 1B, Supplemental Fig. 1). Notably, at the 14 ss *tbx2a* was expressed in a longer domain of the intermediate mesoderm compared to *tbx2b*, which occupied a shorter domain and was expressed weakly in that area (Fig. 1B, C). By the 16 ss, *tbx2a* and *tbx2b* occupied analogous pronephros domains, though *tbx2b* expression was weaker (Fig. 1C). At the 28 ss, or approximately 24 hpf, when segmentation of the pronephros is fully established, transcripts encoding *tbx2a* and *tbx2b* were restricted to the area where the DL and the PD reside within the pronephros (Fig. 1B, Supplemental Fig. 1). As demonstrated by fluorescent *in situ* hybridization at the 28 ss, *tbx2a* and *tbx2b* were co-localized in this distal pronephros area, though the *tbx2b* renal expression domain was slightly broader, and *tbx2a* was more robustly expressed in the posterior duct region (Fig. 1D). These findings suggested that *tbx2a/b* are localized to renal progenitors during nephrogenesis, and specifically implicated them as possible candidates for regulating distal intermediate mesoderm fates such as the DL segment.

Due to the spatial distribution of *tbx2a* and *tbx2b* expression at the 28 ss, we next determined if the transcripts were localized to a particular emergent lineage(s) in the pronephros and/or the CS glands. To assess their presence in the DL, we performed double

fluorescent *in situ* hybridization with *slc12a3*. Transcripts encoding *tbx2a* and *tbx2b* were co-localized to *slc12a3*-expressing cells (Fig. 2A). The CS lineage is situated at the anterior aspect of the DL at this time, being a small group of cells that emerge from the intermediate mesoderm in a location next to the 15th somite (Elizondo et al., 2005; Wingert et al., 2007), which co-express *sim1a* and *stc1* (Fig. 2B). Given this close proximity of the CS and the DL, we assessed expression of *stc1* along with *tbx2a* or *tbx2b* (Fig. 2B). Interestingly, *tbx2a* transcripts were not detectable in *stc1+* cells while all *stc1*-expressing cells were *tbx2b +*(Fig. 2B). These data confirmed our hypothesis that *tbx2a* and *tbx2b* are expressed in the DL at the 28 ss, and revealed that *tbx2b* is also expressed by the CS lineage at this stage.

3.2. tbx2a/b promote the formation of the DL segment

To investigate the possibilities that *tbx2a* and/or *tbx2b* participate in nephron patterning, we next undertook loss of function studies. We utilized gene knockdowns and a *tbx2b* deficient mutant, *fby*^{c144}, which encodes a T-to-A transversion that introduces a premature stop codon within the T-box DNA-binding domain (Snelson et al., 2008). For the knockdowns, previously reported morpholinos (MOs) for *tbx2a*, *tbx2b* and *tbx2a/b* were used that either targeted the start site of the gene or interfered with pre-mRNA splicing (Thu et al., 2013; Gross and Dowling, 2005; Ribeiro et al., 2007; Sedletcaia and Evans, 2011). We used RT-PCR to validate that the use of *tbx2a* and *tbx2b* splice-blocking MOs interrupted splicing activity, which in each case led to some products that are predicted to encode truncated proteins (Supplementary Fig. 2). Although wild-type transcripts were still produced when implementing each splice-blocking MO, the expression of transcripts encoding Tbx2 peptide truncations that remove the 3′-terminal region has been reported to produce dominant-negative effects (Stott et al., 1993; Rao, 1994; Dheen et al., 1999). Therefore, to next assess pronephros development, wild-type embryos were injected at the 1-cell stage, and then morphants and uninjected siblings were fixed at the 28 ss to examine nephron segmentation using double whole mount *in situ* hybridization. To help define alterations in nephron segment pattern formation, we detected transcripts encoding *slow myosin heavy chain 1* (*smyhc1*) to mark the somites.

Interestingly, deficiency of *tbx2a, tbx2b*, or combined *tbx2a/b* loss of function was associated with a reduced distal tubule domain along with an expanded proximal region (Fig. 3). The PCT expresses the gene *solute carrier family 20, member 1a* (*slc20a1a*), in a domain that was situated adjacent to somites 5–8 in wild-type embryos, while *tbx2a, tbx2b*, and *tbx2a/b* morphants exhibited an expansion of this segment, such that the PCT was situated adjacent to somites 5–9 (Fig. 3). In comparison, the PST segment, which can be detected using a riboprobe corresponding to the *transient receptor potential cation channel, subfamily M, member 7* (*trpm7*), was unaffected in size within *tbx2a, tbx2b*, and *tbx2a/b* morphants, but displayed an axial location shift that correlated with the expanded PCT segment domain (Fig. 3). The DE domain was marked by *solute carrier family 12, member 1* (*slc12a1*), which encodes a Na/K/Cl cotransporter, and had a similar length in wild-types and *tbx2a, tbx2b*, and *tbx2a/b* morphants but experienced a one somite distal shift (Fig. 3). The DL domain, marked by the Na/Cl transporter gene *solute carrier family 12, member 3* (*slc12a3*), was consistently reduced in *tbx2a, tbx2b*, and *tbx2a/b* morphants where it was

restricted to a domain located next to somites 15–17, whereas wild-type embryos showed *slc12a3* expression in a domain located next to somites 14–17 (Fig. 3).

To further assess these segment alterations, the absolute lengths of the PCT, PST, DE and DL domains were measured in triplicate cohorts of wild-type controls in addition to *tbx2a*, *tbx2b*, and *tbx2a/b* deficient embryos (Supplemental Fig. 3A). Overall, these phenotypes were penetrant and consistent in the majority of morphant embryos (Supplementary Fig. 3B–G). Of note, we have a robust ability to score the boundaries of the PCT, DE and the DL due to the nature of these respective riboprobes, which are not prone to background staining. By comparison, the *trpm7* riboprobe used to label PST can produce some background. For this reason, PST phenotypes were scored more conservatively than the other segments, but we nevertheless observed 50–60% of *tbx2*-deficient animals with a very clear PST shift. Statistical analysis of these segment lengths confirmed that there was not a significant change in either the PST or DE segments due to single or double *tbx2* knockdown (Supplemental Fig. 3A). In contrast, we found that there was a statistically significant decrease in DL segment length in single and double *tbx2* deficient embryos compared to wild-type controls, as well as an increase in the PCT length associated with *tbx2* loss of function (Supplemental Fig. 3A). We also explored whether double *tbx2* knockdown altered mesodermal patterning. Analysis of several intermediate, paraxial, and lateral plate mesoderm markers suggested that these divisions were normally inculcated by early somitogenesis stages (Supplemental Fig. 4; data not shown).

Next, segment changes were assessed in both the *tbx2b* deficient line fby^{c144} and in fby^{c144} injected with the *tbx2a* splicing MO. In both of these experimental contexts, we found that the loss of *tbx2b* or the combined loss of *tbx2a/b* induced a similar reduction in the DL segment domain, along with an expansion in the PCT segment domain; further, there were corresponding distal shifts in the location of the PST and DE (Fig. 3). Interestingly, approximately 20% of $fby^{c144-/-}$ mutants displayed a normal segment pattern, consistent with partial penetrance of this particular allele—though 50% of $fby^{c144+/-}$ also displayed pronephric and CS phenotypes, which might reflect a dominant negative effect or possibly haploinsufficiency (data not shown).

We conclude from these findings that *tbx2a* and *tbx2b* are required for normal nephron segmentation in the absence of earlier mesoderm patterning events. In light of the expression domain of *tbx2a* and *tbx2b* in the distal IM, we hypothesized that these factors specifically promote DL fate, and that the alterations in PCT formation might be a secondary, i.e. indirect phenotype. Further, the observation that dual loss of *tbx2a* and *tbx2b* resulted in a similar phenotype to either knockdown alone suggested the possibility that they act in the same pathway to influence normal nephron segmentation.

3.3. tbx2a/b act to inhibit the formation of the CS during nephrogenesis

As mentioned previously, the CS, to date found only in bony fishes, are sac-like bodies located adjacent to the kidney. Based on the distal IM expression domains of *tbx2a* and *tbx2b* during early somitogenesis, as well as the specific expression of *tbx2b* in the CS at 28 ss (Fig. 2B), we hypothesized that CS development might also be regulated by one or both of the *tbx2* genes.

To explore this possibility, we performed whole mount *in situ* hybridization on wild-type controls and *tbx2*-deficient embryos to examine expression of the CS marker *stc1*, which enables precise and reliable quantification of CS cell number (Supplemental Fig. 5). In wild-type embryos, the CS possessed an average of 4 cells per nephron (Fig. 4A, B). By comparison, knockdown of *tbx2a, tbx2b*, or both *tbx2a/b* induced an apparent expansion in the size of the CS (Fig. 4A). Likewise, *fby*^{c144} mutant embryos exhibited an increased CS (Fig. 4A). To determine if these changes were due to elevated cell numbers, we quantified CS cell number in *tbx2*-deficient embryos (Fig. 4B). While *tbx2a* knockdown induced a small but significant increase in CS cell number, both *tbx2b* deficient and *tbx2a/b* doubly deficient embryos exhibited a dramatic, approximately three-fold increase in the number of *stc1*$^{+}$ cells (Fig. 4B).

In a previous study, the transcription factor *sim1a* was shown to be necessary and sufficient for the formation of the *stc1*-expressing CS lineage (Cheng and Wingert, 2015). Notably, *sim1a* expression precedes that of *stc1*, as it is expressed in CS precursors at the 24 ss, while *stc1* is expressed in CS cells beginning at the 28 ss (Cheng and Wingert, 2015). Therefore, we next investigated whether *tbx2*-deficiency affected CS formation by influencing the expression of *sim1a*. To do this, whole mount *in situ* hybridization was utilized to assess the spatiotemporal expression domain of *sim1a* in the context of *tbx2a*, *tbx2b* and dual *tbx2a/b* deficiency. Here, we found that the number of *sim1a+* CS cells was significantly increased in *tbx2a, tbx2b*, and *tbx2a/b* deficient animals (Fig. 4C, D). Taken together, this data suggests that *tbx2a/b* are factors that inhibit CS formation, most likely by limiting the expression of *sim1a* and consequently affecting the number of *stc1*$^{+}$ cells that develop to form the CS lineage.

3.4. tbx2a/b are necessary and sufficient to promote DL formation and inhibit the CS

To determine whether increased levels of *tbx2a* and/or *tbx2b* transcripts were sufficient to induce changes in nephron cell identity, we injected wild-type embryos with *tbx2a* or *tbx2b* capped RNA (cRNA). Overexpression of either *tbx2a* or *tbx2b* resulted in a one somite expansion in the *slc12a3*-expressing DL segment at a minimum cRNA dose of 50 pg and a maximum dose of 750 pg (Fig. 5A). There was no observed change in the PCT, PST, or DE segments upon injection of 500 pg/nL of *tbx2a* or *tbx2b* cRNA (Supplementary Fig. 6). Testing at additional doses of 50, 100, 250, or 1000 pg/nL *tbx2a* or *tbx2b* cRNA also failed to initiate changes in these segments (data not shown).

To further assess segment alterations after *tbx2a* or *tbx2b* overexpression, the absolute lengths of the PCT, PST, DE and DL domains were measured (Fig. 5D; Supplemental Fig. 6B). Statistical analysis of these segment lengths confirmed that there was not a significant change in the PCT, PST or DE due to alterations in *tbx2a/b* (Supplemental Fig. 6A).
To assess how the DL expansion aligned with the adjacent DE segment, we performed double fluorescent *in situ* hybridization with the markers *slc12a3* and *slc12a1* (Fig. 5B). This revealed that there was co-mingling of distinct *slc12a1+* and *slc12a3+* cells in the pronephros region situated adjacent to somite 13 (Fig. 5B). These data indicated that the expansion of *slc12a3+* cells populating this area was actually mosaic after *tbx2a* or *tbx2b*

overexpression, and thus resolve how an expansion of the DL domain occurred while the DE domain was unchanged.

Next, we performed rescue studies using cRNA paired with *tbx2a* or *tbx2b* splice targeting MOs to verify that the observed DL segment changes seen in our morphants were specifically due to loss of *tbx2a* or *tbx2b*, respectively, and to test if *tbx2b* could specifically rescue *fby*^{c144} mutant embryos. We observed a normal DL in ~40% of *tbx2a* MO + *tbx2a* cRNA and ~50% *tbx2b* MO + *tbx2b* cRNA embryos, as well as *fby*^{c144} mutants + *tbx2b* cRNA, compared to the 2–3% wild-type phenotype observed in embryos injected with either cRNA or MO alone, which was based on measurements of absolute length of the DL (Fig. 5C, D, Supplementary Fig 7A).

We also examined CS development using whole mount *in situ* hybridization to detect *stc1* transcripts following overexpression of either *tbx2a* or *tbx2b* (Fig. 6). Addition of either *tbx2a* cRNA or *tbx2b* cRNA resulted in a significantly lower number of CS cells (Fig. 6A, B). This difference further suggests that both *tbx2* factors have potent downstream consequences that can restrict CS development. With these morpholino knockdown studies, we also assessed the ability of *tbx2a* or *tbx2b* overexpression to specifically rescue the expansion of the CS lineage, and the ability of *tbx2b* to rescue CS ontogeny in *fby*^{c144}. Approximately 60% of *tbx2a/b* MO + *tbx2a/b* cRNA injected embryos had a wild-type CS with between 3 and 7 cells associated with each nephron (Fig. 6A, B, Supplementary Fig 7B). Quantification of the CS cells revealed that there were no significant differences in cell number between *tbx2a* rescues and wild-type, *tbx2b* rescues and wild-type, or *tbx2a* rescues and *tbx2b* rescues (Fig. 6B). Taken together, the compilation of our various loss of function, overexpression and rescue studies demonstrate that *tbx2a/b* are necessary and sufficient to promote the formation of the DL and suppress the formation of the CS.

3.5. tbx2a is epistatic to tbx2b during DL and CS development, and likely has other targets

Given the intriguing observation that the expression of *tbx2a* transcripts in the distal IM slightly precede the expression of *tbx2b* in this region, and the finding that the combined loss of *tbx2a/b* function led to identical outcomes as either factor alone, we hypothesized that they may occupy a shared pathway in which *tbx2a* does indeed predicate *tbx2b*. To explore this, we examined the expression domains of *tbx2a* and *tbx2b* transcripts in *tbx2b* and *tbx2a* morphants, respectfully (Fig. 7A, B). The knockdown of *tbx2b* was not associated with any alteration in the *tbx2a* pronephros expression domain at the 28 ss compared to wild-type control embryos (Fig. 7A). In contrast, *tbx2a* knockdown was linked to a reduced *tbx2b* expression domain in the distal pronephros at the 28 ss compared to wild-type embryos (Fig. 7B). Measurements of the absolute lengths of these *tbx2a* and *tbx2b* domains, followed by statistical analysis, confirmed that the nephron expression domain of *tbx2b* was significantly reduced in *tbx2a* morphants compared to wild-types, and that there was no difference in *tbx2a* expression between *tbx2b* morphants and wild-type embryos (Fig. 7C). The restriction of the *tbx2b* expression domain in *tbx2a* morphant embryos at the 28 ss suggested that *tbx2b* transcripts were lost in the developing CS (Fig. 7B). To confirm this specifically, we performed double fluorescent *in situ* hybridization studies in *tbx2a* morphant embryos to examine the spatial localization of both *tbx2b* and *stc1* transcripts (Fig. 7D).

We found that *stc1+* cells lacked *tbx2b* transcripts (Fig. 7D) in *tbx2a* deficient embryos, consistent with the model that *tbx2a* knockdown leads in part to the loss of *tbx2b* expression in the CS lineage.

Next, we performed rescue studies to determine whether overexpression of *tbx2b* or *tbx2a* was sufficient to ameliorate the CS and DL phenotypes caused by *tbx2a* or *tbx2b* loss of function, respectfully (Fig. 7E–H; Supplemental Fig. 7). The overexpression of *tbx2b* rescued the CS expansion and DL reduction in close to or exceeding a majority of *tbx2a* morphants, where approximately 40% of embryos had a wild-type DL and approximately 70% a wild-type CS (Fig. 7E, Supplemental Fig. 7). This data is consistent with the conclusion that *tbx2b* acts downstream of *tbx2a*.

Surprisingly, however, overexpression of *tbx2a* also rescued the CS expansion and DL reduction in some *tbx2b* morphants, though the frequency of the rescue was comparatively less, with approximately 30% of embryos showing a wild-type DL and 20% a wild-type CS (Fig. 7G, Supplemental Fig. 7). Given the multiple lines of evidence that suggest *tbx2b* acts downstream of *tbx2a*, our interpretation of these findings is that *tbx2a* promotes the DL and inhibits the CS through one or more alternative targets as well.

3.6. RA regulates both tbx2a and tbx2b during zebrafish nephrogenesis

RA signaling has previously been established as both a critical activator and suppressor of segment patterning in the zebrafish pronephros (Wingert et al., 2007; Wingert and Davidson, 2011; Li et al., 2014; Cheng and Wingert, 2015; Marra and Wingert, 2016). In wild-type embryos, RA acts as a morphogen to promote the formation of proximal segments at the expense of distal segments. When RA concentrations are low or absent, only the formation of distal segments occurs. Thus, the early-acting RA chemical gradient creates the diversity of segments seen in the zebrafish nephron. In previous studies, *sim1a* was placed downstream of RA signaling, as its domain was altered by chemical treatments with exogenous RA or the RA biosynthesis inhibitor, 4-diethylaminobenzaldehyde (DEAB) (Cheng and Wingert, 2015). Since *tbx2a/b* also alter the *sim1a* domain, we aimed to investigate the relationship between RA and *tbx2a/b*. To determine this, wild-type embryos were treated with exogenous RA concentrations between 1×10^{-6} M and 1×10^{-8} M from 90% epiboly to the 28 ss, or with DEAB at a concentration of 1.6×10^{-5} M starting at either 50% or 90% epiboly until the 28 ss.

After performing whole mount *in situ* hybridization on chemically treated embryos and controls using probes for *tbx2a* and *tbx2b*, we found that RA and DEAB treatments do alter the *tbx2a/b* expression domains (Fig. 8). The minimum RA concentration for effects appeared to be 1×10^{-8} M. At 1×10^{-7} M, the pronephric expression domains of both *tbx2a* and *tbx2b* was reduced to just the duct/cloaca region, and at 1×10^{-6} M RA, pronephric expression of *tbx2a* and *tbx2b* was abolished (Fig. 8). Reciprocally, the domains of both *tbx2a* and *tbx2b* expression were expanded in embryos that had been treated with DEAB at both 50% and 90% epiboly (Fig. 8). The phenotypes observed in these drug-treated embryos were highly penetrant and consistent across replicates (Supplementary Fig. 8).

These results are consistent with the notion that the expression of *tbx2a* and *tbx2b* tracks with the DL and the CS, as the expression of these genes correlates with the previous observations of reduction and expansion of the DL segment and the CS during ectopic RA addition and RA inhibition by DEAB, respectively (Wingert et al., 2007; Wingert and Davidson, 2011). While these observations are consistent with the interpretation that *tbx2a* and *tbx2b* are each negatively regulated by RA signaling during nephrogenesis, these experiments do not establish whether the interaction is direct or indirect.

3.7. Notch signaling and tbx2a/b cooperate to repress CS development in the zebrafish

Several studies have demonstrated essential roles of the Notch signaling pathway, downstream of RA signaling, in mediation of the renal progenitor fate decisions during nephron pattern formation (Cheng and Kopan, 2005; Cheng et al., 2007; Georgas et al., 2009). For example, there is evidence that RA acts upstream of Notch to mediate cell fate choice within the pronephros (Li et al., 2014; Marra and Wingert, 2016), which led us to hypothesize that the activities of *tbx2a*, *tbx2b* and *sim1a* that occur downstream of RA might interface or somehow collaborate with Notch signaling to regulate CS development. Therefore, we next explored the involvement of Notch signaling in CS differentiation in nephrogenesis.

To do this, we utilized the double transgenic line *Tg(hsp70::GAL4, UAS::NICD)* to ectopically activate Notch signaling through heat-shock induction at the 15 ss. Conversely, to block the Notch signaling pathway, wild-type embryos were treated with 100 μm of the gamma-secretase inhibitor DAPT at 90% epiboly through the 28 ss. Surprisingly, ectopic activation of Notch resulted in a striking reduction in CS formation in the transgenic embryos, while wild-type siblings underwent normal CS development (Fig. 9A). In contrast, DAPT-treated wild-type embryos had a significantly expanded CS (Fig. 9A). Again, alterations in the size of the CS were due to changes in the number of $stc1^{+}$ cells, as shown by cell number quantification (Fig. 9B). These data suggest that Notch also acts to inhibit CS formation during zebrafish nephrogenesis in a pattern similar to loss and gain of *tbx2a/b*.

To investigate whether *tbx2a/b* cooperates with Notch in regulation of the CS, we performed MO knockdown of *tbx2a/b* in NICD embryos and then performed heat-shock induction at 15 ss. Interestingly, whereas *tbx2a/b* morphant siblings showed an increased number of cells which expressed markers of the CS lineage, activated NICD-*tbx2a/b* morphants failed to show a reduction in CS formation that is characteristic of uninjected activated NICD mutants (Fig. 9). In addition, *tbx2a/b* morphants as well as fby^{c144} mutant embryos were subjected to DAPT chemical treatments to block Notch signaling. While a CS expansion was evident, the effects of blocking both Notch and *tbx2a/b* or *tbx2b* were not significantly different than inhibiting either of these components alone (Fig. 9). The inability of *tbx2a/b* absence to rescue the diminished CS of heat-shocked NICD embryos or additively increase the CS clusters of DAPT-treated embryos suggests that *tbx2a/b* function downstream of Notch signaling in a common pathway to suppress CS differentiation.

4. Discussion

Knowledge of the complex genetic requirements for successful nephron segment formation in zebrafish has a number of applications in developmental biology and regenerative medicine. Here, our work has illuminated the requirement for two previously unexplored genetic participants during the process of nephron segmentation: *tbx2a* and *tbx2b.* Additionally, we have found a new role for these genes, along with the Notch signaling pathway, during the specification of the CS.

Our observations that the expression of *tbx2a* and *tbx2b* transcripts is restricted to the caudal renal progenitors led us to hypothesize that these genes play a part in segment patterning of the distal pronephros, and possibly formation of the CS. Indeed, loss of function studies resulted in a decrease in the DL segment, and overexpression of either *tbx2a* or *tbx2b* was sufficient to expand the DL, which lead us to conclude that the actions of both factors promote the formation of the DL segment (Fig. 10). As *tbx2a/b* are not expressed proximally, it seems reasonable to surmise that the expansion of the PCT segment during *tbx2* deficiency is a secondary consequence of the DL alteration. The mechanism(s) by which this occurs is(are) extremely intriguing to contemplate. Understanding the regulation of cellular dynamics in the context of nephron segment patterning, as well as elucidating if and how adjacent subtypes of renal progenitors interact, are just two avenues for investigation that are likely to provide vital clues. Next, while our epistasis experiments indicate that *tbx2a* is upstream of *tbx2b*, they also suggest *tbx2a* mitigates the DL and CS lineages by regulating an additional target(s). The identification of these mystery components, and determination of where they fit in the working model of nephrogenesis (Fig. 10) are very important areas for continued research. Further, our results have led us to hypothesize that part of the mechanism for how RA negatively regulates the DL during nephrogenesis occurs is through its negative regulation of the *tbx2a* and *tbx2b* expression domains. However, the present study does not resolve whether RA signaling directly or indirectly regulates *tbx2* genes, and as such this is another important point for subsequent work.

We also discovered that *tbx2a/b* and the Notch signaling pathways repress CS development, providing key formative insights into the genetic components that influence this poorly characterized lineage. Noticeably, *tbx2a/b* deficient embryos formed significantly larger CS clusters, as shown by the elevated number of *stc1* and *sim1a* expressing cells. A similar CS expansion was seen when Notch signaling was blocked using DAPT. Notch overexpression also led to a depression in CS formation. As knockdown of *tbx2a/b* in NICD transgenic embryos failed to repress CS formation post heat-shock induction, and DAPT-treated *tbx2a/b* morphants exhibited no additional CS expansion, we conclude that *tbx2a/b* act downstream of Notch to inhibit CS development (Fig. 10). More studies are needed to decipher the relationship between *tbx2a/b* with each other, as well as how these factors interact with particular Notch pathway components, during segment patterning and CS formation.

4.1. The roles of Tbx2 in development and tbx2a/b functions in patterning the pronephros

The vertebrate T-box gene family, which arose from a single primeval gene in a common metazoan ancestor, consists of over 17 transcription factors that are now appreciated to play many roles in animal development (Abrahams et al., 2010). Tbx2 belongs to the Tbx2 subfamily (which includes Tbx3, Tbx4, and Tbx5) and is expressed in numerous tissues during embryogenesis, including endoderm and mesoderm derivatives such as the lung and kidney, respectively (Bollag et al., 1994; Chapman, et al., 1996). Tbx2 is a potent suppressor of transcription, though an activation domain has also been identified, suggesting that the protein may have versatile roles (Paxton et al., 2002; Abrahams et al., 2010). Indeed, Tbx2 is involved in a multitude of events. For example, elegant genetic studies have established that mammalian Tbx2 has distinct roles during heart development (Harrelson et al., 2004; Cai et al., 2005), eye development (Behesti et al., 2009), lung growth (Ludtke, et al., 2013), limb field specification and posterior digit identity (Isaac et al., 1998; Logan et al., 1998; Suzuki et al., 2004; Nissim et al., 2007), and mammary gland development (Douglas and Papaioannou, 2013)—just to name a few.

Consequent to the teleost genome duplication, zebrafish have retained two *tbx2* genes, which share 79.5% peptide identity (Sedletcaia and Evans, 2011). To date, both redundant and unique roles have been attributed to the zebrafish *tbx2a* and *tbx2b* paralogs: *tbx2a* has a distinct role in regulating morphogenesis of the pharyngeal arches (Thu et al., 2013), while *tbx2b* is required for development of the pineal organ (Snelson et al., 2008), and both *tbx2a/b* are functionally redundant for regulating heart chamber development (Sedletcaia and Evans, 2011).

With respect to vertebrate kidney development, *Tbx2* was detected in total RNA from the adult murine kidney (Bollag et al., 1994). The spatiotemporal expression of *Tbx2* during renal development of the mouse has been described previously in the mesonephros and meta-nephric tubules at E12.5 (Chapman et al., 1996). Additionally, *Tbx2* transcripts have been detected in the Wolffian (mesonephric) duct of developing mouse embryos, as well as in the ureteric bud tips of the collecting duct system during branching morphogenesis of the meta-nephric kidney (GUDMAP: 10896). In light of this and the present findings, exploring the functional role of Tbx2 in mammalian kidney will be important in future studies. Tbx2 null murine embryos die due to their cardiovascular defects, which has precluded analysis of its function in renal development (Harrelson et al., 2004), though a conditional null allele has been created that could be invaluable for further analyses (Wakker et al., 2010). As we have observed that the zebrafish *tbx2* homologs, *tbx2a* and *tbx2b*, are both expressed in a region of the distal pronephros which consists of both DL and a purported partially overlapping PD segment, an interesting hypothesis for prospective studies is that *tbx2a/b* have conserved roles in PD/collecting duct development as well. At present, exploration of this possibility is currently limited by a paucity of molecular markers of the zebrafish PD, but advances might be achieved by targeted expression profiling of these cells or through the assessment of other genes expressed in the ureteric bud tips.

Despite the conservation in *tbx2* expression in the renal duct networks among various organisms, the molecular mechanisms underlying how *tbx2* impacts kidney development continue to be unresolved. In tadpoles, overexpressing *Tbx2* inhibited nephric mesoderm

formation and *Tbx2* transcripts were localized to the non-nephric mesenchyme of the IM that surrounds the nephric anlage (Cho et al., 2011). In contrast, *Tbx2* inactivation expanded the boundary of the pronephric nephron, resulting in an enlarged pronephros (Cho et al., 2011). These results implied that *Tbx2* plays a role in determining the size of the pronephros territory (Cho et al., 2011). Unlike these findings, alterations of *tbx2a/b* levels during zebrafish pronephric development did not alter pronephros size but led to changes in nephron segment pattern.

While the role of *Tbx2* in mammalian nephrogenesis remains to be determined, the observed conservation in renal expression across vertebrates suggests the possibility that *Tbx2* participates in mammalian kidney organogenesis in a way similar to zebrafish by promoting distal segment and/or collecting duct formation. Whether alterations in Tbx2 are linked to human renal congenital abnormalities or other diseases may be a valuable area for future study. Additional work to understand the molecular consequences of alterations in *tbx2a/b* using the zebrafish may provide a useful model to explore these aspects, as has been the case for a number of other genetic alterations (Poureetezadi and Wingert, 2016).

4.2. tbx2a/b and induction of the CS in teleosts

The CS has been characterized for its secretion of Stanniocalcin (STC), a homodimeric glycoprotein hormone with an integral role in calcium and phosphate homeostasis in fishes (McCudden et al., 2001). STC in fish acts to prevent hyperkalemia and is released into the bloodstream in response to serum Ca^{2+} elevations, whereas in the kidney it stimulates phosphate reabsorption in order to balance excess Ca^{2+} in the serum (Lu et al., 1994). Interestingly, the mammalian counterparts of this protein, STC1 and STC2, are found in low levels in blood serum but their subcellular functions remain to be resolved (Yeung et al., 2011). Despite relatively intensive studies on the CS gland and STC, not much is known about how the CS is formed and what molecular mechanisms regulate its differentiation.

Recent findings by our lab have identified the transcription factor *sim1a* as a critical modulator of CS differentiation, as disrupting *sim1a* function completely abrogated the formation of *stc1*-expressing cells of the CS in the zebrafish pronephros (Cheng and Wingert, 2015). Our data has added further knowledge on the regulation of CS development during zebrafish nephrogenesis. Due to our observations that *stc1* and *sim1a* are co-localized in CS cells at the 28 ss, we postulate that *sim1a* is another viable marker to examine the CS at this time point. In addition, loss of *tbx2a/b* resulted in a significant increase in the number of CS cells, which was detected by an increase in cells expressing *stc1* and *sim1a.* This places *tbx2a/b* as an upstream repressor of *sim1a*, which leads to suppression of CS development. This model is further strengthened by our data that overexpression of *tbx2a/b* caused a drop in the number of CS cells. Interestingly, as a patterning factor, *sim1a* is also involved in negotiating the PCT/PST boundary (Cheng and Wingert, 2015). As our studies demonstrate that *tbx2a/b* negatively regulate *sim1a*, this could provide an explanation for the expansion of the PCT upon loss of *tbx2a/b* which could be tested experimentally in future studies.

4.3. Notch signaling pathway is also involved in CS regulation during zebrafish nephrogenesis

Previous studies in mammalian models demonstrated the crucial role of the Notch signaling pathway in effecting cell fate decisions in the mammalian nephron (Cheng et al., 2003, 2007; Cheng and Kopan, 2005). In the zebrafish pronephros, studies have shown that Notch signaling inhibits the formation of multiciliated cells (MCCs) to advance transporter cell fates such as the PST (Liu et al., 2007; Ma and Jiang, 2007; Marra et al., 2016). While the cellular lineages of the CS have not yet been extensively characterized, we hypothesized that Notch could be involved in regulating CS formation. Chemically inhibiting Notch signaling with DAPT resulted in an increase in the numbers of CS cells in embryos. Conversely, ectopically activating Notch via our NICD heat-shock transgenic line resulted in an almost complete loss of CS cells. We have therefore identified Notch signaling as a suppressor of CS development in the zebrafish pronephros. This novel role for Notch signaling is important for continuing to comprehend how this critical developmental pathway functions in the zebrafish pronephros and its associated tissues.

In addition to reporting *tbx2a/b* and Notch signaling as repressors of CS development, we also provide baseline information about how these factors are positioned within the network of CS regulatory genes. Loss of *tbx2a/b* paired with loss and gain of Notch lead to CS cell number increases that was comparable to loss of *tbx2a/b* alone. This indicates that *tbx2a/b* act downstream of Notch signaling to suppress the CS. Whether this relationship involves direct activation by Notch or a cascade of intermediates is currently unknown, thus future studies will focus on resolving the mechanistic details of this interaction.

4.4. The links between nephrogenesis and kidney disease

In this study, we identified the T-box transcription factors *tbx2a* and *tbx2b* as crucial regulators of nephron patterning, where they may also possibly act to regulate renal progenitor differentiation during zebrafish nephrogenesis. The specification and patterning of the nephron progenitor is a complex process that requires integrative regionalization of each progenitor population, as highly specialized nephron epithelial cells made in each domain carry out distinct physiological functions. Whereas applications of zebrafish and other models such as amphibians continue to advance the knowledge of nephrogenesis (Desgrange and Cereghini, 2015), a large gap nevertheless remains regarding the broad picture of the molecular control behind renal progenitor specification. Understanding the genetic, molecular, and cellular mechanisms of nephrogenesis has far reaching implications for kidney diseases ranging from congenital anomalies of the kidney and urinary tract (CAKUT) to acquired renal injuries because a common aspect that unifies kidney diseases with diverse pathologies is the loss of function or dysfunction of nephrons. The rising incidence of kidney disease and limitations for treatment pose ongoing medical challenges (Saran et al., 2015). Discoveries of the key modulators during nephron patterning and the molecular mechanisms underlying renal progenitor commitment are needed to better understand the processes of nephrogenesis and kidney ontogeny to help create new, innovative regenerative therapeutics. As researchers continue to endeavor to cultivate renal precursors, through emergent techniques like organoid culture (Chambers et al., 2016), the information collected from the analysis of simplified nephron models such as the vertebrate

pronephros can continue to assist in illuminating lineage relationships and gene regulatory networks.

Supplementary Material

Refer to Web version on PubMed Central for supplementary material.

Acknowledgments

This work was supported in part by NIH Innovator Grant DP2OD008470 and NIH Grant R01DK100237 to RAW, as well as by National Science Foundation Graduate Research Fellowships DGE-1313583 awarded to BED and ANM. RAW thanks MBS & FG for their support. We are grateful to Elizabeth and Michael Gallagher for their generous gift to the University of Notre Dame for the support of stem cell research. The funders had no role in the study design, data collection and analysis, decision to publish, or manuscript preparation. We are also indebted to Drs. Jim Patton and Dominic Didiano, as well as Mr. Simon Wu, at Vanderbilt University, for kindly providing the *fby*^{c144} mutant line for these studies. This study used data from the GUDMAP database http://www/gudmap.org [5/2016], including expression data from entry (GUDMAP: 10896, Contributed by E. Lesieur, K. Georgas, B. Rumballe, H.S. Chiu, R. Thiagarajan, D. Taylor, K. Chawengsaksophak, M. Little, P. Koopman, S. Grimmond). We thank the staffs of the Department of Biological Sciences and Center for Stem Cells and Regenerative Medicine, and particularly express our gratitude to staff of the Center for Zebrafish Research at the University of Notre Dame for their dedication and care of our zebrafish aquarium. Finally, we thank the members of our lab for their support, discussions, and insights about this work.

Appendix A. Supporting information

Supplementary data associated with this article can be found in the online version at doi:10.1016/j.ydbio.2016.10.019.

Abbreviations

cRNA
capped RNA

CS
corpuscle of Stannius

DAPT
N-[N-(3,5-difluorophenacetyl)-L-alanyl]-S-phenylglycine t-butyl ester

DEAB
4-diethylaminobenzaldehyde

DE
distal early

DL
distal late

***fby*^{c144}**
from beyond

hpf
hours post fertilization

IM
intermediate mesoderm

NICD
Tg(hsp70::Gal4, UAS::NICD

MO
morpholino

N
neck

P
podocytes

PCT
proximal convoluted tubule

PD
pronephric duct

PST
proximal straight tubule

PD
pronephric duct

RA
retinoic acid

sim1a
single-minded family bHLH transcription factor 1a

slc12a1
solute carrier family 12, member 1

slc12a3
solute carrier family 12, member 3

slc20a1a
*solute carrie*r family 20, member 1a

smyhc1
slow myosin heavy chain 1

ss
somite stage

stc1
stanniocalcin 1

tbx2a
t-box 2a

tbx2b
t-box 2b

trpm7
transient receptor potential cation channel, subfamily M, member 7

References

Abrahams A, Parker MI, Prince S. 2010; The T-box transcription factor Tbx2: its role in development and possible implication in cancer. IUBMB Life. 62 :92–102. [PubMed: 19960541]

Behesti H, Papaioannou VE, Sowden JC. 2009; Loss of Tbx2 delays optic vesicle invagination leading to small optic cups. Dev Biol. 333 :360–372. [PubMed: 19576202]

Bollag RJ, Siegfried Z, Cebra-Thomas JA, et al. 1994; An ancient family of embryonically expressed mouse genes sharing a conserved protein motif with the T locus. Nat Genet. 7 :383–388. [PubMed: 7920656]

Brend T, Holley SA. 2009; Zebrafish whole mount high-resolution double fluorescent in situ hybridization. J Vis Exp. (25) :1229. [PubMed: 19322135]

Cai CL, Zhou W, Yang L, et al. 2005; T-box genes coordinate regional rates of proliferation and regional specification during cardiogenesis. Development. 132 :2475–2487. [PubMed: 15843407]

Chambers JM, McKee RM, Drummond BD, et al. 2016; Evolving technology: creating kidney organoids from stem cells. AIMS Bioeng. 3 :305–318. [PubMed: 28393110]

Chang AC, Janosi J, Hulsbeek M. 1995; A novel human cDNA highly homologous to the fish hormone stanniocalcin. Mol Cell Endocrinol. 112 :241–247. [PubMed: 7489828]

Chapman DL, Garvey N, Hancock S, et al. 1996; Expression of the T-box family genes, Tbx1-Tbx5, during early mouse development. Dev Dyn. 206 :379–390. [PubMed: 8853987]

Cheng CN, Li Y, Marra AN, et al. 2014; Flat mount preparation for observation and analysis of zebrafish embryo specimens stained by whole mount in situ hybridization. J Vis Exp. (89) :51604.

Cheng, CN, Wingert, RA. Chapter 9: renal system development in the zebrafish: a basic nephrogenesis model. In: Carver, E, Lessman, C, editors. Zebrafish: Topics in Reproduction & Development. Nova Scientific Publishers; 2014. 179–214.

Cheng CN, Wingert RA. 2015; Nephron proximal tubule patterning and corpuscles of Stannius formation are regulated by the sim1a transcription factor and retinoic acid in zebrafish. Dev Biol. 399 :100–116. [PubMed: 25542995]

Cheng HT, Miner J, Lin M, et al. 2003; Gamma-Secretase activity is dispensable for the mesenchyme-to-epithelium transition but required for proximal tubule formation in developing mouse kidney. Development. 130 :5031–5041. [PubMed: 12952904]

Cheng HT, Kopan R. 2005; The role of Notch signaling in specification of podocyte and proximal tubules within the developing mouse kidney. Kidney Int. 68 :1951–1952. [PubMed: 16221173]

Cheng HT, Kim M, Valerius MT. 2007; Notch2, but not Notch1, is required for proximal fate acquisition in the mammalian nephron. Development. 134 :801–811. [PubMed: 17229764]

Cho GS, Choi SC, Park EC, et al. 2011; Role of Tbx2 in defining the territory of the pronephric nephron. Development. 138 :465–474. [PubMed: 21205791]

Costantini F, Kopan R. 2010; Patterning a complex organ: branching morphogenesis and nephron segmentation in kidney development. Dev Cell. 18 :698–712. [PubMed: 20493806]

Dheen T, Sleptsova-Friedrich I, Xu Y, et al. 1999; Zebrafish tbx-c functions during formation of midline structures. Development. 126 :2703–2713. [PubMed: 10331981]

Desgrange A, Cereghini S. 2015; Nephron patterning: lessons from Xenopus, zebrafish and mouse studies. Cells. 4 :483–499. [PubMed: 26378582]

Douglas NC, Papaioannou VE. 2013; The T-box transcription factors TBX2 and TBX3 in mammary gland development and breast cancer. J Mammary Gland Biol Neoplasia. 18 :143–147. [PubMed: 23624936]

Dressler GR. 2006; The cellular basis of kidney development. Annu Rev Cell Dev Biol. 22 :509–529. [PubMed: 16822174]

Drummond BE, Wingert RA. 2016; Insights into kidney stem cell development and regeneration using zebrafish. World J Stem Cells. 8 :22–31. [PubMed: 26981168]

Ebarasi L, Oddsson A, Hultenby K, et al. 2011; Zebrafish: a model system for the study of vertebrate renal development, function, and pathophysiology. Curr Opin Nephrol Hypertens. 20 :416–424. [PubMed: 21519251]

Elizondo MR, Arduini BL, Paulsen J, et al. 2005; Defective skeletogenesis with kidney stone formation in dwarf zebrafish mutant for trpm7. Curr Biol. 15 :667–671. [PubMed: 15823540]

Garrett FD. 1942; The development and phylogeny of the corpuscles of Stannius in ganoid and teleostean fishes. J Morphol. 70 :41–67.

Georgas K, Rumballe B, Valerius MT. 2009; Analysis of early nephron patterning reveals a role for distal RV proliferation in fusion to the ureteric tip via a cap mesenchyme-derived connecting segment. Dev Biol. 322 :273–286.

Gerlach GF, Wingert RA. 2013; Kidney organogenesis in the zebrafish: insights into vertebrate nephrogenesis and regeneration. Wiley Interdiscip. Rev Dev Biol. 2 :559–585. [PubMed: 24014448]

Gerlach GF, Wingert RA. 2014; Zebrafish pronephros tubulogenesis and epithelial identity maintenance are reliant on the polarity proteins Prkc iota and zeta. Dev Biol. 396 :183–200. [PubMed: 25446529]

Gross JM, Dowling JE. 2005; tbx2b is essential for neuronal differentiation along the dorsal/ventral axis of the zebrafish retina. PNAS. 102 :4371–4376. [PubMed: 15755805]

Harrelson Z, Kelly RG, Goldin SN, et al. 2004; Tbx2 is essential for patterning the atrioventricular canal and for morphogenesis of the outflow tract during heart development. Development. 131 :5041–5052. [PubMed: 15459098]

Isaac A, Rodriquez-Esteban C, Ryan A. 1998; Tbx genes and limb identity in chick embryo development. Development. 125 :1867–1875. [PubMed: 9550719]

Kaneko T, Hasegawa S, Hirano T. 1992; Embryonic origin and development of the corpuscles of Stannius in chum salmon (*Oncorhynchus keta*). Cell Tissue Res. 268 :65–70. [PubMed: 1499053]

Kimmel CB, Ballard WW, Kimmel SR, et al. 1995; Stages of embryonic development of the zebrafish. Dev Dyn. 203 :253–310. [PubMed: 8589427]

Krishnamurthy VG. 1976; Cytophysiology of corpuscles of Stannius. Int Rev Cytol. 46 :177–249. [PubMed: 186426]

Kroeger PT, Wingert RA. 2014; Using zebrafish to study podocyte genesis during kidney development and regeneration. Genesis. 52 :771–792. [PubMed: 24920186]

Lengerke C, Wingert R, Beeretz M, et al. 2011; Interactions between Cdx genes and retinoic acid modulate early cardiogenesis. Dev Biol. 163 :134–142.

Li Y, Cheng CN, Verdun VA, et al. 2014; Zebrafish nephrogenesis is regulated by interactions between retinoic acid, mecom, and Notch signaling. Dev Biol. 386 :111–122. [PubMed: 24309209]

Little MH, McMahon AP. 2012; Mammalian kidney development: principles, progress and projections. Cold Spring Harb Perspect Biol. 4 :a008300. [PubMed: 22550230]

Liu Y, Narendra P, Kramer-Zucker A, et al. 2007; Notch signaling controls the differentiation of transporting epithelia and multiciliated cells in the zebrafish pronephros. Development. 134 :1111–1122. [PubMed: 17287248]

Logan M, Simon HG, Tabin C. 1998; Differential regulation of T-box and homeobox transcription factors suggests roles in controlling chick limb-type identity. Development. 125 :2825–2835. [PubMed: 9655805]

Lu M, Wagner GF, Renfro JL. 1994; Stanniocalcin stimulates phosphate reabsorption by flounder renal proximal tubule in primary culture. Am J Physiol. 267 :R1356–R1362. [PubMed: 7977865]

Ludtke THW, Farin HF, Rudat C, et al. 2013; Tbx2 controls lung growth by direct repression of the cell cycle inhibitor genes Cdkn1a and Cdkn1bb. PLoS Genet. 9 :e1003189. [PubMed: 23341776]

Ma M, Jiang YJ. 2007; Jagged2a-Notch signaling mediates cell fate choice in the zebrafish pronephric duct. PLoS Genet. 3 :e18. [PubMed: 17257056]

Marra AN, Wingert RA. 2014; Roles of Iroquois transcription factors in kidney development. Cell Dev Biol. 3 :131.

Marra AN, Wingert RA. 2016; Epithelial cell fate in the nephron tubule is mediated by the ETS transcription factors *etv5a* and *etv4* during zebrafish kidney development. Dev Biol. 411 :231–245. [PubMed: 26827902]

Marra AN, Li Y, Wingert RA. 2016; Antennas of organ morphogenesis: the roles of cilia in vertebrate kidney development. Genesis. 54 :457–469. [PubMed: 27389733]

McCudden CR, Kogon MR, DiMattia GE, Wagner GF. 2001; Novel expression of the stanniocalcin gene in fish. J Endocrinol. 171 :33–44. [PubMed: 11572788]

McKee R, Gerlach GF, Jou J, et al. 2014; Temporal and spatial expression of tight junction genes during zebrafish pronephros development. Gene Expr Patterns. 16 :104–113. [PubMed: 25460834]

Miceli R, Kroeger PT Jr, Wingert RA. 2014; Molecular mechanisms of podocyte development revealed by zebrafish kidney research. Cell Dev Biol. 3 :138.

Naylor RW, Przepiorski A, Ren Q, et al. 2013; HNF1B is essential for nephron segmentation during nephrogenesis. J Am Soc Nephrol. 24 :77–87. [PubMed: 23160512]

Nissim S, Allard P, Bandyopadhyay A, et al. 2007; Characterization of a novel ectodermal signaling centre regulating Tbx2 and Shh in the vertebrate limb. Dev Biol. 304 :9–21. [PubMed: 17300775]

O'Brien LL, Grimaldi M, Kostun Z, et al. 2011; Wt1a, Foxc1a, and the Notch mediator Rbpj physically interact and regulate the formation of podocytes in zebrafish. Dev Biol. 358 :318–330. [PubMed: 21871448]

Paxton C, Zhao H, Chin Y, et al. 2002; Murine Tbx2 contains domains that activate and repress gene transcription. Gene. 283 :117–124. [PubMed: 11867218]

Poureetezadi SJ, Wingert RA. 2016; Little fish, big catch: zebrafish as a model for kidney disease. Kidney Int. 89 :1203–1209.

Rao Y. 1994; Conversion of a mesodermalizing molecule, the Xenopus Brachyury gene, into a neuralizing factor. Genes Dev. (8) :939–947. [PubMed: 7926778]

Ribeiro I, Kawakami Y, Büscher D, et al. 2007; Tbx2 and Tbx3 regulate the dynamics of cell proliferation during heart remodeling. PLoS One. 25 :e398.

Romagnani P, Lasagni L, Remuzzi G. 2013; Renal progenitors: an evolutionary conserved strategy for kidney regeneration. Nat Rev Nephrol. 9 :137–146. [PubMed: 23338209]

Saxen, L. Organogenesis of the Kidney. Cambridge University Press; Cambridge, UK: 1987.

Saran R, Li Y, Robinson B, et al. 2015; US Renal Data System 2014 annual data report: epidemiology of kidney disease in the United States. Am J Kidney Dis. 66 :S1–S306.

Scheer N, Campos-Ortega JA. 1999; Use of the Gal4-UAS technique for targeted gene expression in the zebrafish. Mech Dev. 80 :153–158. [PubMed: 10072782]

Scheer N, Riedl I, Warren JT, et al. 2002; A quantitative analysis of the kinetics of Gal4 activator and effector gene expression in the zebrafish. Mech Dev. 112 :9–14. [PubMed: 11850174]

Sedletcaia A, Evans T. 2011; Heart chamber size in zebrafish is regulated redundantly by duplicated tbx2 genes. Dev Dyn. 240 :1548–1557. [PubMed: 21448936]

Slanchev K, Putz M, Schmitt A, et al. 2011; Nephrocystin-4 is required for pronephric duct-dependent cloaca formation in zebrafish. Hum Mol Gen. 20 :3119–3128. [PubMed: 21596840]

Snelson CD, Santhakumar K, Halpern ME, et al. 2008; tbx2b is required for the development of the parapineal organ. Development. 135 :1693–1702. [PubMed: 18385257]

Stott D, Kispert A, Herrmann B. 1993; Rescue of the tail defect of Brachyury mice. Genes Dev. 7 :197–203. [PubMed: 8436292]

Suzuki T, Takeuchi J, Koshiba-Takeuchi T, et al. 2004; Tbx genes specify posterior digit identity through Shh and BMP signaling. Dev Cell. 6 :43–53. [PubMed: 14723846]

Takasato M, Little ML. 2015; The origin of the mammalian kidney: implications for recreating the kidney in vitro. Development. 142 :1937–1947. [PubMed: 26015537]

Thisse, B; Thisse, C. Fast Release Clones: A High Throughput Expression Analysis. ZFIN Direct Data Submission. 2004. ⟨http://zfin.org⟩

Thu HN, Tien SF, Loh SL, et al. 2013; *tbx2a* is required for specification of endodermal pouches during development of the pharyngeal arches. PLoS One. 8 :e77171. [PubMed: 24130849]

Wagner GF, Guiraudon CC, Milliken C. 1995; Immunological and biological evidence for a stanniocalcin-like hormone in the human kidney. PNAS. 92 :1871–1875. [PubMed: 7892193]

Wakker V, Brons JF, Aanhaanen WTJ, et al. 2010; Generation of mice with a conditional null allele for Tbx2. Genesis. 48 :195–199. [PubMed: 20095052]

Westerfield, M. The Zebrafish Book. University of Oregon Press; Eugene, OR, USA: 1993.

Wingert RA, Selleck R, Yu J, et al. 2007; The cdx genes and retinoic acid control the positioning and segmentation of the zebrafish pronephros. PLoS Genet. 3 :1922–1938. [PubMed: 17953490]

Wingert RA, Davidson AJ. 2008; The zebrafish pronephros: a model to study nephron segmentation. Kidney Int. 73 :1120–1127. [PubMed: 18322540]

Wingert RA, Davidson AJ. 2011; Zebrafish nephrogenesis involves dynamic spatiotemporal expression changes in renal progenitors and essential signals from retinoic acid and irx3b. Dev Dyn. 240 :2011–2027. [PubMed: 21761484]

Yeung BHY, Law AYS, Wong CKC. 2011; Evolution and roles of stanniocalcin. Mol Cell Endocrinol. 349 :272–280. [PubMed: 22115958]

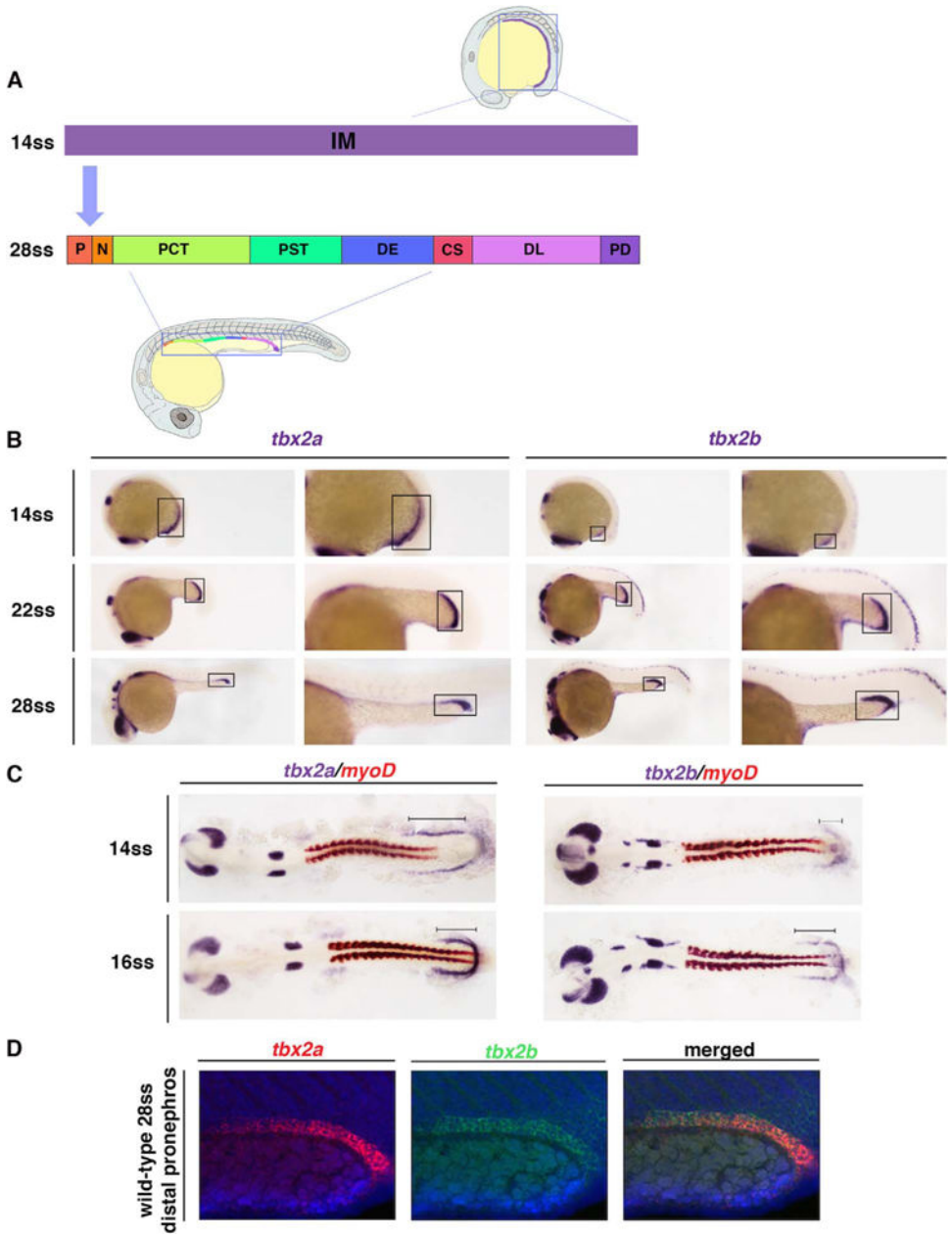

Fig. 1.

tbx2a/b transcripts are specifically expressed in the caudal domain of the renal progenitor field during nephrogenesis. (A) Schematic of zebrafish pronephros development. The intermediate mesoderm (IM) gives rise to the two-nephron pronephros, which is fully segmented by 24 hpf (28 ss): P (podocytes), N (neck), PCT (proximal convoluted tubule), PST (proximal straight tubule), DE (distal early tubule), CS (corpuscle of Stannius), DL (distal late tubule) and PD (pronephric duct). (B) Whole mount *in situ* hybridization shows that *tbx2a* and *tbx2b* transcripts are expressed in the distal region of the pronephros. At 14 ss, *tbx2a* transcripts can be detected in the distal region of the intermediate mesoderm while *tbx2b* transcripts are observed in a smaller distal domain. At 22 ss, *tbx2b* expression in the distal pronephros closely resembles *tbx2a* expression in this region. However, by 28

ss, *tbx2a* transcripts are most intensely expressed in the PD segment and trail off in the DL segment, while *tbx2b* transcripts are evident throughout the DL and more sparsely in the PD. (C) Flatmount images of embryos co-stained with *tbx2a* and *myoD*, and *tbx2b* and *myoD* show that *tbx2a* is more widely expressed in the emergent distal pronephros than *tbx2b* at 14 ss. At 16 ss, *tbx2b* expression expands and begins to resemble *tbx2a* expression. (D) Fluorescent *in situ* hybridization shows that *tbx2a* and *tbx2b* are co-expressed in portions of the PD and DL at 28 ss. Specifically, *tbx2a* is expressed more intensely in the PD than *tbx2b.* In addition, *tbx2b* has a stronger expression in the DL, while *tbx2a* expression begins to taper off.

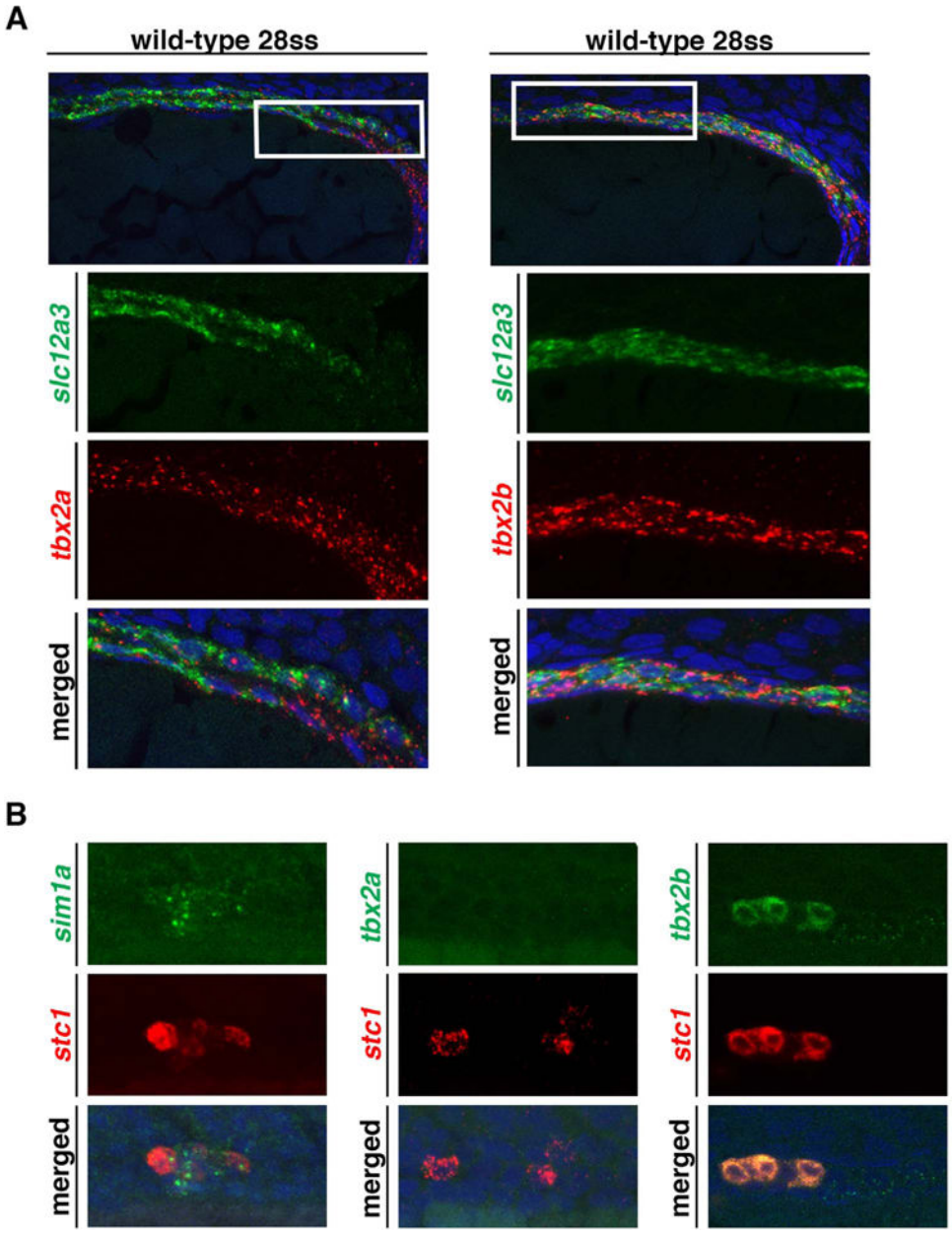

Fig. 2.

tbx2a/b exhibit co-expression with the DL and CS. (A) Fluorescent *in situ* hybridization was used to examine the distal region of the pronephros of wild-type 28 ss embryos, with DAPI (blue) used to label nuclei. *tbx2a* expression again appears strongest in the PD segment and fades as it progresses anteriorly. The region in the white box represents the moderate co-expression seen between *tbx2a* and *slc12a3* near the boundary of the *slc12a3* domain. In contrast, *tbx2b* expression appears strongly co-localized through most of the length of the DL, as exemplified by the region in the white box. In addition, *tbx2b* continues to be expressed past the DL in the PD segment. (B) The transcription factor *sim1a*, which has been demonstrated to be a necessary requirement for CS formation, shows specific co-localization with CS marker *stc1* in wild-type, 28 ss embryos. This indicates that *sim1a*

can be used as a secondary indicator for changes in the CS. Additionally, when examining the CS in wild-type embryos at 28 ss it was noted that *tbx2a* is not expressed in or near the CS while *tbx2b* does co-localize with *stc1* in the CS at this stage.

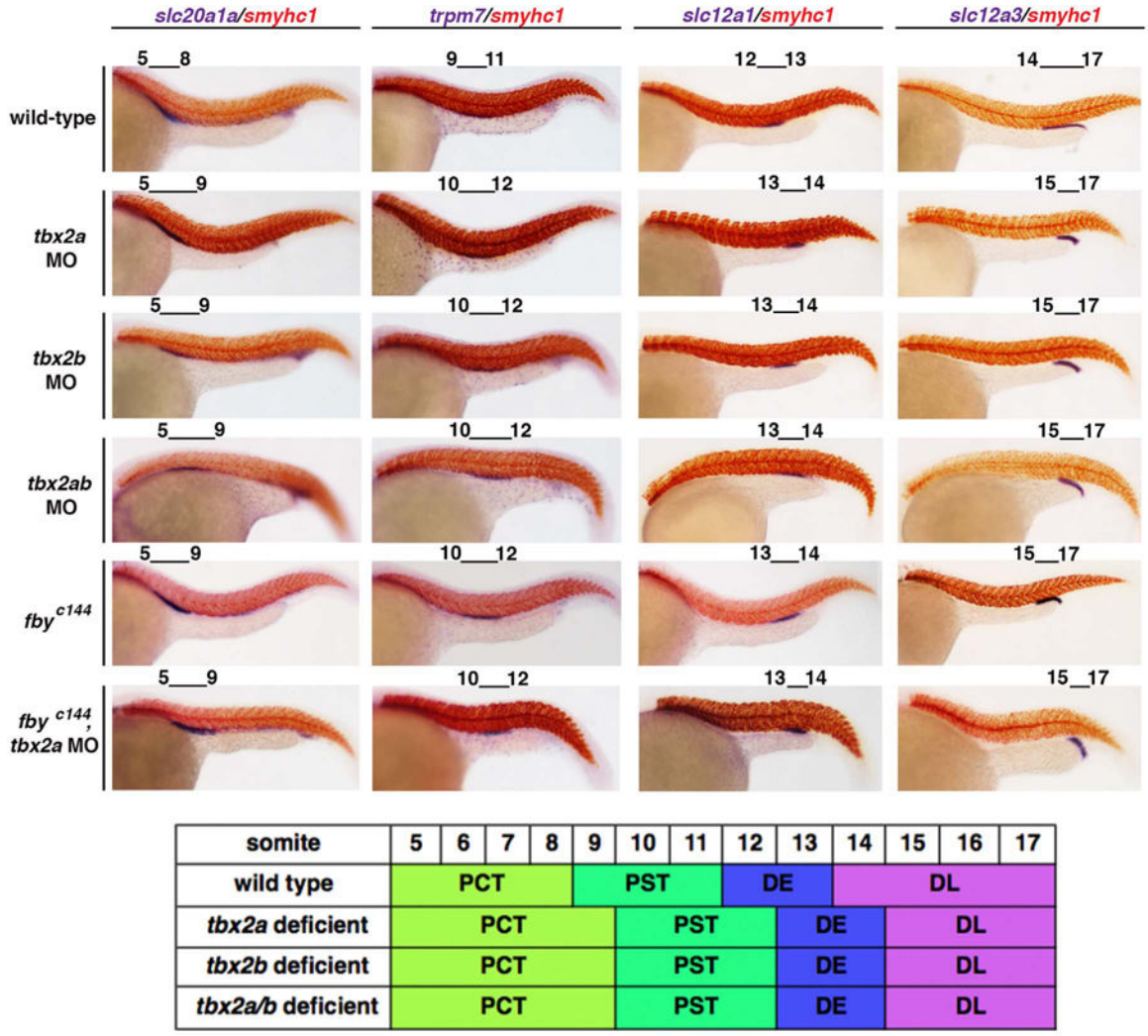

somite	5	6	7	8	9	10	11	12	13	14	15	16	17
wild type	PCT				PST			DE		DL			
tbx2a deficient	PCT					PST			DE		DL		
tbx2b deficient	PCT					PST			DE		DL		
tbx2a/b deficient	PCT					PST			DE		DL		

Fig. 3.

tbx2a/b deficiency leads to a decrease in the size of the DL segment and a slight expansion in the PCT segment in the pronephros. Upper panel: At 28 ss, double whole mount *in situ* hybridization was used to label segmental domains in wild-type and *tbx2a/b* deficient embryos. Somites were labeled using *smyhc1* (red) to detect length changes in adjacent pronephros segments (purple). Within proximal domains, MO knockdown of *tbx2a, tbx2b*, or *tbx2a/b* induced a 1-somite expansion in the *slc20a1a*-expressing PCT segment in morphant pronephros. This same expansion was also seen in *fby*^{c144} mutants (*tbx2b* deficient) and *fby*^{c144} mutants injected with *tbx2a* MO. Within distal domains, *tbx2a/b* deficient morphants and mutants exhibited a 1–2 somite reduction in the *slc12a3*-expressing DL segment at 24 hpf. The PST and DE segments, labeled by transcripts encoding *trpm7* and *slc12a1*, respectively, exhibited a 1 somite posterior shift in *tbx2a/b* deficient embryos compared to wild-type embryos due to changes in the domain size of the PCT and DL segments. Representative wild-type and morphant results are based on somite counting of at least 20 embryos per marker. In *fby*^{c144} embryos, segments showed consistent changes based on somite counting of at least 3 genotype-confirmed mutants per marker. Lower panel:

Schematic summary of pronephros segment organization in wild-type and *tbx2a/b* deficient embryos. Abbreviations: PCT (proximal convoluted tubule), PST (proximal straight tubule), DE (distal early tubule), DL (distal late tubule) and MO (morpholino).

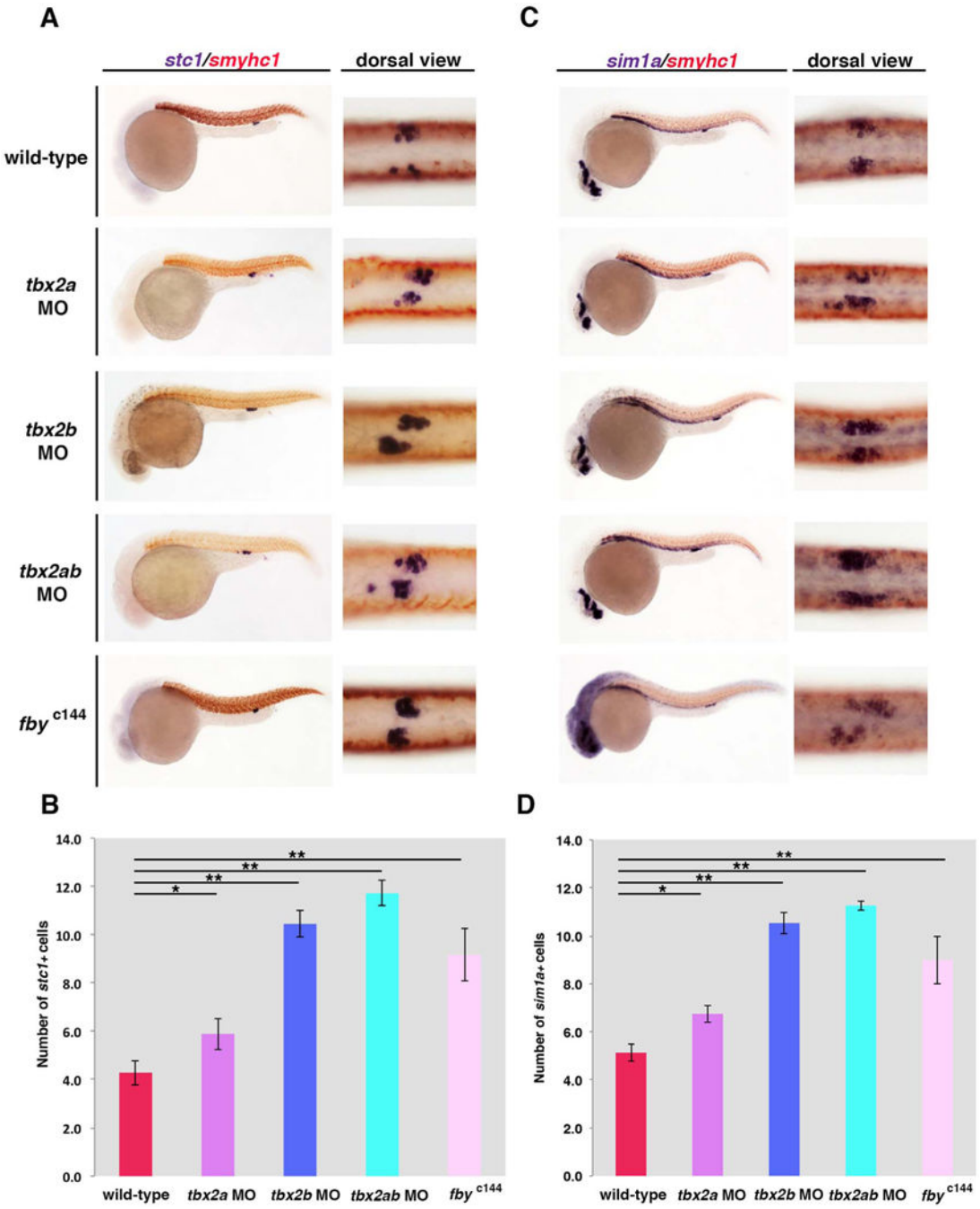

Fig. 4.

tbx2a/b deficiency leads to an increase in the number of cells in the CS. (A) The CS was labeled by whole mount *in situ* hybridization to detect transcripts encoding *stc1* at the 28 ss stage. (B) In wild-type embryos, each CS is typically comprised of about 4–6 $stc1^{+}$ cells per nephron. However, *tbx2a/b* deficiency in morphants and fby^{c144} mutants induced a significant increase of the $stc1^{+}$ cell number in the CS. (C) Labeling the CS with *sim1a* revealed a similar phenotype consistent with an inhibitory role of *tbx2a/b* in CS development. (D) Quantification of *sim1a+* CS cell number revealed that *tbx2a, tbx2b*

and *tbx2a/b* morphants and *fby*^{c144} mutants all led to a significantly greater number of CS cells than wild-type embryos. For each experiment, at least 15 morphant embryos and 3 genotypically confirmed *fby*^{c144} mutant embryos were examined. (*$p < 0.05$, **$p < 0.001$). Abbreviations: CS (corpuscle of Stannius).

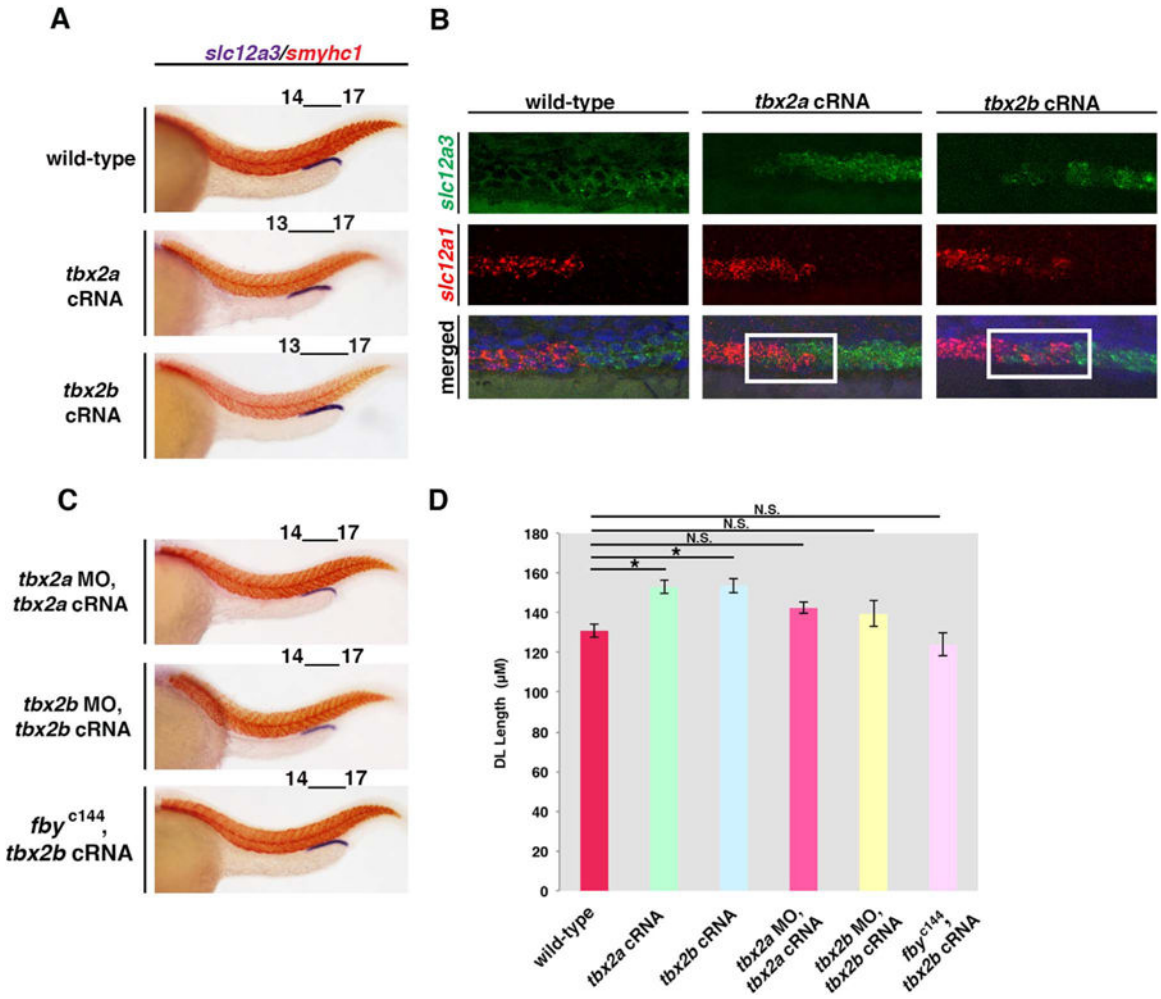

Fig. 5.

tbx2a/b are necessary and sufficient to promote the formation of the DL. (A) Injecting wild-type embryos with either *tbx2a* or *tbx2b* cRNA resulted in a significant expansion of the DL as observed by somite counting (*smyhc1*). (B) In wild-type, 28 ss embryos, the DL (*slc12a3*) domain and the DE (*slc12a1*) domain are distinctive. In embryos overexpressing either *tbx2a* or *tbx2b*, DE cells and DL cells appear to be co-mingled adjacent to the 13th somite. This observation explains why the DL expands to the 13th somite in *tbx2a/b* overexpressing embryos but the DE, PST, and PCT domains remain unaltered. DAPI (blue) was used to label nuclei (C) Rescue studies reveal that DL domain changes in *tbx2a* and *tbx2b* morphants are specific to loss of *tbx2a* and *tbx2b*, rather than toxicity. Wild-type embryos were co-injected with either *tbx2a* cRNA and *tbx2a* ATG MO or *tbx2b* cRNA and *tbx2b* ATG MO. In addition, fby^{c144} mutants were injected with *tbx2b* cRNA. In all treatments, a wild-type DL was observed some of the time as indicated by somite counting and length measurements. (D) The DL of 5 embryos from each overexpression and rescue treatment was measured in uM. A significant increase in the DL was seen in animals injected with *tbx2a* cRNA and *tbx2b* cRNA, but no significant change in DL length was observed in any of the rescue experimental parameters. (*$p < 0.05$, **$p < 0.001$, N.S. = not significant). Abbreviations: cRNA (capped RNA), MO (morpholino), DL (distal late).

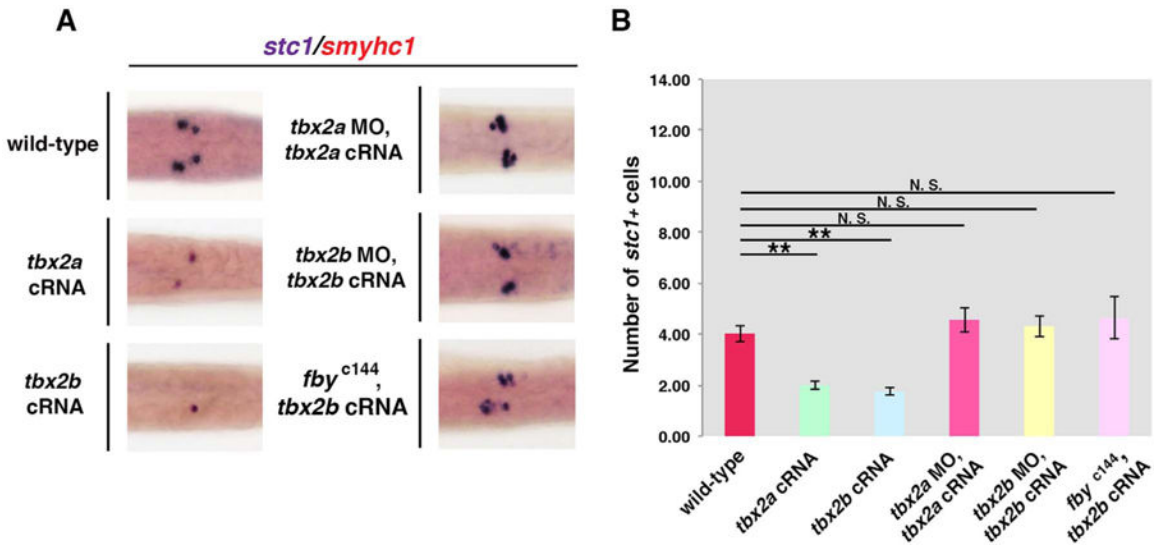

Fig. 6.

tbx2a/b are necessary and sufficient to inhibit CS cellular expansion. (A) Dorsal images of wild-type 28 ss embryos injected with *tbx2a* and *tbx2b* cRNA show that *tbx2a/b* overexpression results in a decrease in the number of *stc1*-expressing CS cells. Rescue studies were conducted by co-injecting wild-type with either *tbx2a* cRNA and *tbx2a* MO or *tbx2b* cRNA and *tbx2b* MO and fby^{c144} mutants with *tbx2b* cRNA. In all three conditions, the CS was successfully rescued. (B) The number of CS cells in each nephron was counted for at least 10 representative embryos from each condition. The number of CS cells in embryos injected with *tbx2a* cRNA and *tbx2b* cRNA were significantly lower than wild-type embryos. In contrast, the number of CS cells in rescue study embryos was not significantly different than wild-type embryos. (*$p < 0.05$, **$p < 0.001$, N.S.=not significant). Abbreviations: cRNA (capped RNA), CS (corpuscle of Stannius).

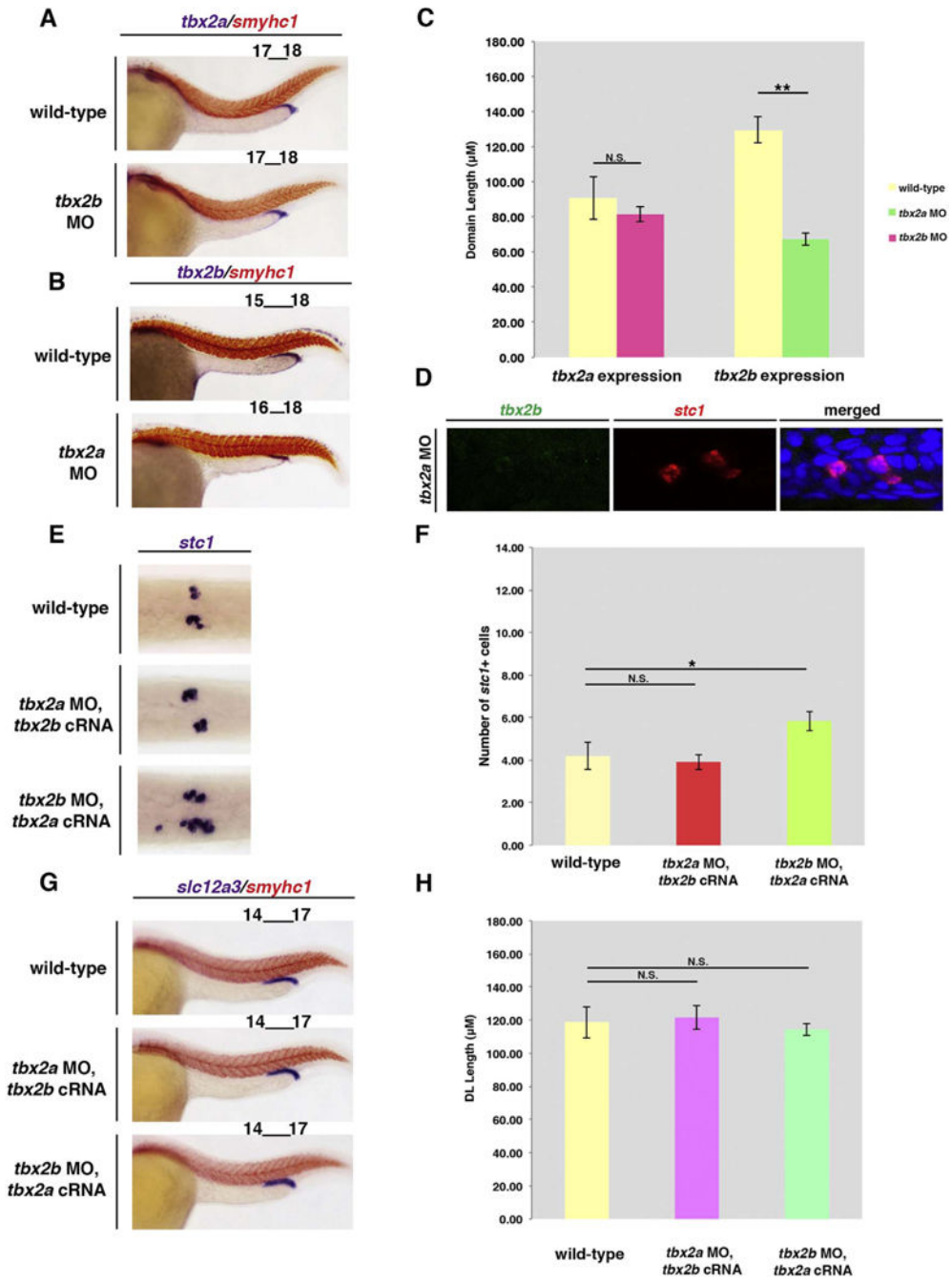

Fig. 7.

tbx2a functions upstream of *tbx2b* during pronephros segment and CS development. (A, B) Whole mount *in situ* hybridization was performed with *tbx2a* probe on 28 ss wild-type embryos and embryos injected with *tbx2b* MO. The *tbx2a* domain remained the same somite length despite the loss of *tbx2b*. In contrast, loss of *tbx2a* caused a notable decrease in the *tbx2b* domain. (C) The length of *tbx2a* and *tbx2b* expression domains of five representative embryos was measured (uM). While *tbx2a* expression is not significantly different wild-type and *tbx2b* morphants, the size of the *tbx2b* domain is significantly smaller than their wild-

type siblings. (D) Fluorescent *in situ* hybridization was used to examine the distal region of the pronephros of *tbx2a* morphant embryos at the 28 ss, which revealed that *stc1*+ CS cells lacked *tbx2b* transcripts. DAPI (blue) was used to label nuclei. (E, F) A portion of embryos injected with *tbx2b* MO and *tbx2a* cRNA exhibited a normal number of CS cells, but the average number of CS cells was significantly larger than the wild-type controls. A more robust rescue was seen in embryos injected with *tbx2a* MO and *tbx2b* cRNA, which on average had a similar number of CS cells compared to wild-type embryos. (G, H) DL lengths were rescued in some embryos by *tbx2a* cRNA in *tbx2b* morphants, and by *tbx2b* cRNA in *tbx2a* morphants, such that the average DL lengths were not significantly different from wild-type controls. (F, H) CS cells and DL lengths were counted in each nephron in 10 individuals in each treatment. (*$p < 0.05$, **$p < 0.001$, N.S.=not significant). Abbreviations: MO (morpholino), cRNA (capped RNA), DL (distal late), CS (corpuscle of Stannius).

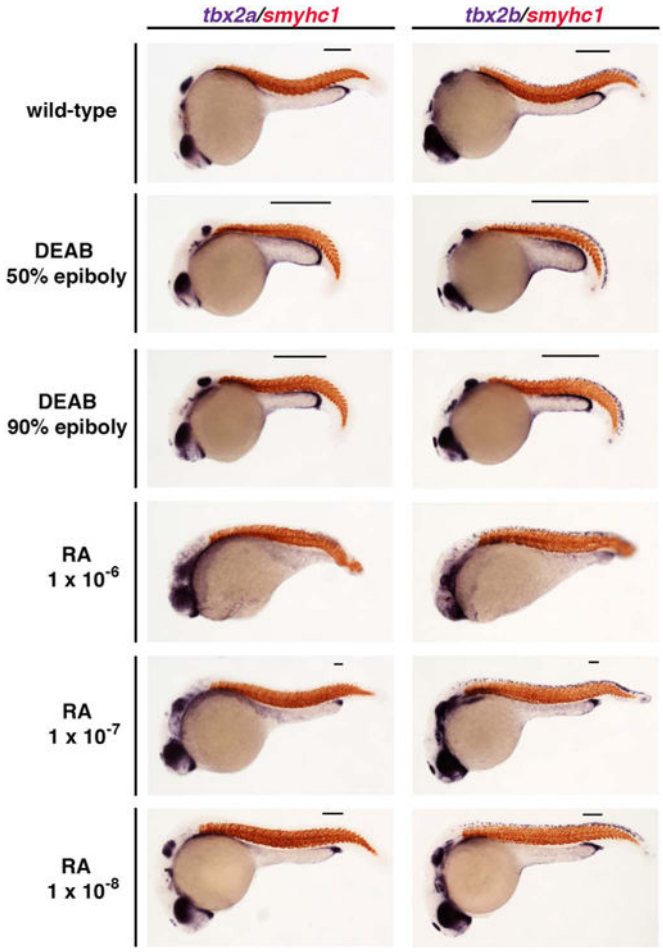

Fig. 8.

tbx2a/b are downstream of retinoic acid in the nephrogenesis pathway. Wild-type embryos were treated with exogenous RA at 3 dosages from 90% epiboly to the 28 ss. Wild-type embryos were also subjected to an RA inhibitor (DEAB) at 1.6×10^{-7} M at either 50% epiboly or 90% epiboly until fixation at 24 hpf. Whole mount *in situ* hybridization was then performed using riboprobes for *tbx2a* and *tbx2b.* Both the *tbx2a* and *tbx2b* domains decreased with at all three doses of RA, with total abrogation of expression occurring at 1×10^{-6} M. In contrast, DEAB treatment induced an expansion in the *tbx2a/b* domains at both treatment time points. This suggests that RA negatively regulates *tbx2a/b* expression, either directly or indirectly, in the development of the distal pronephros. At least 20 representative embryos were examined in each treatment.

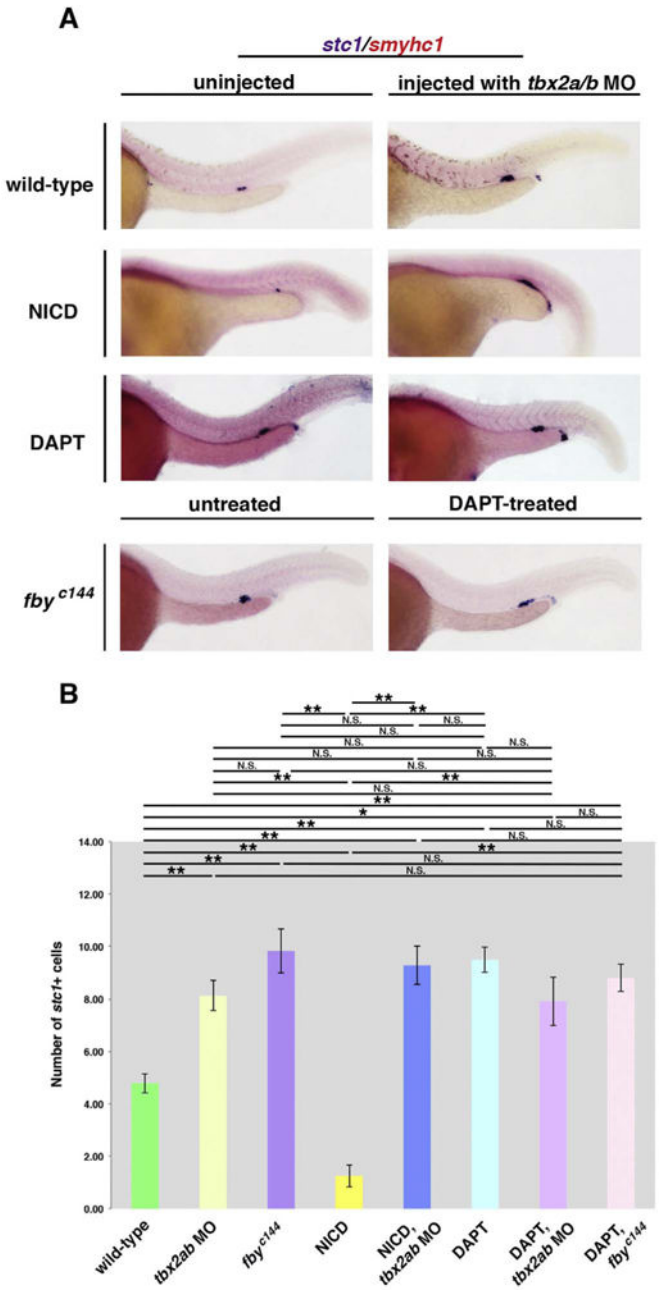

Fig. 9.

Notch signaling also inhibits CS differentiation, but in an upstream or independent way than *tbx2a/b*. NICD embryos were heat-shocked at 15 ss to ectopically activate Notch signaling and fixed at 24 hpf. Post heat-shock induction, NICD embryos exhibited a dramatic reduction of the CS, while siblings showed normal CS clusters. To block Notch signaling, wild-type embryos were incubated in 100 μm DAPT/E3 solution from 90% epiboly to the 24 hpf stage. DAPT treatment resulted in a significant elevation in the number of CS cells. Heat-shocked NICD *tbx2a/b* morphants exhibited a significant expansion in the CS that was in contrast to the reduced CS observed in uninjected heat-shocked NICD siblings. The number of cells in the these CS clusters was not significantly different to the expansion

seen in wild-type embryos injected with *tbx2a/b* MO. DAPT-treated *tbx2a/b* morphants and *fby*^{c144} mutants exhibited an expansion in the CS that was not significantly different than wild-type embryos treated with DAPT alone. Together, these results suggest that *tbx2a/b* are acting in the same pathway, downstream of Notch to suppress the CS. Representative images were based on thorough examination of at least 15 embryos per treatment. (*$p < 0.05$, **$p < 0.001$, N.S.=not significant).

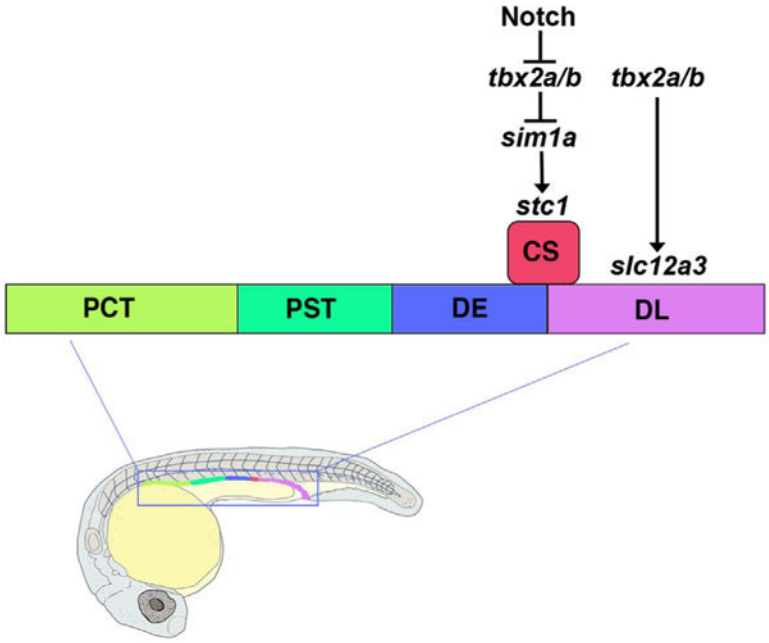

Fig. 10.

Working model. (A) During zebrafish nephrogenesis, the *tbx2a/b* transcription factors regulate patterning of the distal pronephros by promoting DL fate and inhibiting the CS lineage. This is done in part through *tbx2a* regulation of *tbx2b*, though additional targets of *tbx2a* are likely involved as well. CS formation is inhibited by *tbx2a/2b* negative regulation of *sim1a*, which is required for progression of *stc1+* CS cell development. *tbx2a/b* are in turn acting downstream of the Notch signaling pathway to negatively regulate the CS. Abbreviations: PCT (proximal convoluted tubule), PST (proximal straight tubule), DE (distal early tubule), DL (distal late tubule) and CS (corpuscle of Stannius).